โครงการ
การเรียนการสอนเพื่อเสริมประสบการณ์

ชื่อโครงการ	การวิเคราะห์การปิดกั้นของรอยเลื่อน แหล่งจัสมิน บริเวณตอนเหนือของแอ่งปัตตานี อ่าวไทย
ชื่อนิสิต	นางสาวชุติมณฑน์ ภักดีสิโรตม์
ภาควิชา	ธรณีวิทยา
ปีการศึกษา	2558

คณะวิทยาศาสตร์ จุฬาลงกรณ์มหาวิทยาลัย

FAULT SEAL ANALYSIS IN JASMINE FIELD, NORTHERN PART OF PATTANI BASIN, GULF OF THAILAND

MISS CHUTIMON PAKDEESIROTE

A REPORT SUBMITTED IN PARTIAL FULFILLMENT OF THE REQUIREMENTS
FOR THE DEGREE OF THE BACHELOR OF SCIENCE IN GEOLOGY
DEPARTMENT OF GEOLOGY, FACULTY OF SCIENCE, CHULALONGKORN
UNIVERSITY ACADEMIC YEAR 2015

การวิเคราะห์การปิดกั้นของรอยเลื่อน แหล่งจัสมิน บริเวณตอนเหนือของแอ่งปัตตานี อ่าวไทย

นางสาวชุติมณฑน์ ภักดีสิโรตม์

รายงานนี้เป็นส่วนหนึ่งของการศึกษาตามหลักสูตรปริญญาวิทยาศาสตรบัณฑิต
ภาควิชาธรณีวิทยา คณะวิทยาศาสตร์ จุฬาลงกรณ์มหาวิทยาลัย
ปีการศึกษา 2558

Date of submit _____/_____/_____

Date of approve _____/_____/_____

_____

(Dr. Kruawun Jankeaw)

Senior Project Advisor

หัวข้องานวิจัย	การวิเคราะห์การปิดกั้นของรอยเลื่อน แหล่งจัสมิน บริเวณตอนเหนือของแอ่งปัตตานี อ่าวไทย
ผู้ทำการวิจัย	นางสาวชุติมณฑน์ ภักดีสิโรตม์
อาจารย์ที่ปรึกษา	อาจารย์ ดร. เครือวัลย์ จันทร์แก้ว
ที่ปรึกษาร่วม	คุณแองเจล่า เอคาโนฟ, คุณราห์มัท อุโตโน่ และ คุณเธียรพันธุ์ อำไพวรรณ (บริษัท มูบาดาลา ปิโตรเลียม (ประเทศไทย) จำกัด)
ปีการศึกษา	2558

บทคัดย่อ

งานวิจัยนี้มีจุดประสงค์เพื่อวิเคราะห์และประเมินประสิทธิภาพการปิดกั้นไฮโดรคาร์บอนตามระนาบรอยเลื่อนในแหล่งจัสมิน ซึ่งอยู่ทางบริเวณตอนเหนือของแอ่งปัตตานีในอ่าวไทย โดยใช้ข้อมูลคลื่นไหวสะเทือน และข้อมูลการหยั่งธรณีหลุมเจาะของชั้นทรายกักเก็บไฮโดรคาร์บอนที่มีความหนาประมาณ 1680 ฟุต (512 เมตร) มาใช้ในการสร้างแผนที่โครงสร้างทางธรณี, แผนที่ความหนาของชั้นทราย, อัลลัน ไดอะแกรม และคำนวณอัตราส่วนผงรอยเลื่อน รวมทั้งวิเคราะห์ข้อมูลอื่นๆ เพื่อประเมินถึงศักยภาพในการปิดกั้นของรอยเลื่อน

จากการวิเคราะห์อัลลัน ไดอะแกรม พบว่ารอยเลื่อนในแหล่งจัสมินมีประสิทธิภาพในการเป็นตัวปิดกั้นและทำให้เกิดการสะสมตัวของไฮโดรคาร์บอนในบริเวณที่มีการสัมผัสกันของชั้นหินต่างชนิด แต่ในบางบริเวณพบแนวโน้มที่จะเกิดการรั่วไหลของไฮโดรคาร์บอนถ้าทั้งสองด้านของรอยเลื่อนเป็นชั้นทราย จากการคำนวณอัตราส่วนผงรอยเลื่อนประกอบกับการวิเคราะห์ความแตกต่างของความดันข้ามรอยเลื่อน พบว่ามีค่าอยู่ในช่วงที่ทำให้เกิดการปิดกั้นไฮโดรคาร์บอน

วิธีการและผลลัพธ์ที่ได้จากงานวิจัยนี้สามารถนำไปใช้ทำนายประสิทธิภาพและความสามารถในการเป็นตัวปิดกั้นไฮโดรคาร์บอนของรอยเลื่อนในพื้นที่อื่นๆ ที่มีลักษณะธรณีวิทยาและโครงสร้างที่คล้ายคลึงกัน เพื่อใช้สำหรับการวางแผนการผลิตในอนาคตได้

คำสำคัญ: การปิดกั้นของรอยเลื่อน, แหล่งจัสมิน, แอ่งปัตตานี, อัลลัน ไดอะแกรม, อัตราส่วนผงรอยเลื่อน

Title FAULT SEAL ANALYSIS IN JASMINE FIELD, NORTHERN PART OF PATTANI BASIN, GULF OF THAILAND

Researcher Miss. Chutimon Pakdeesirote

Advisor Dr. Kruawun Jankaew

Co-advisor Miss. Angela Echanove, Mr. Rahmat Utono and Mr. Tianpan Ampaiwan (Mubadala Petroleum (Thailand) Limited)

Academic year 2015

ABSTRACT

The Jasmine Field is located in the Northern part of Pattani Basin, Gulf of Thailand. The objective of this study is to analyze and evaluate the possibility of fault sealing in the Jasmine A area by using well data and seismic interpretation from selected reservoir sand horizons, within a total interval thickness of approximately 1680 ft (512 m). These data were used for constructing depth structure maps, net-sand (isopach) maps, the model cross section of Allan diagram and Shale Gouge Ratio (SGR) calculation. In addition, these data were also used to investigate potential of fault sealing.

From Allan diagram, the two analyzed faults in Jasmine A area have an effective capacity in sealing hydrocarbon and can be the entrapment of hydrocarbon accumulation in the area with different juxtaposed units. However, some sections have leakage potential where each horizon is juxtaposed against one another across the fault. As seen in the SGR calculation and the across-fault pressure difference estimation, the results confirm seal capacity and show the threshold for static hydrocarbon sealing. Furthermore, the methodology and the result in this research can be applied to predict the fault seal capacity in other areas of similar lithologies and structures and help to evaluate the potential in hydrocarbon accumulation.

Keywords: Fault sealing, Jasmine Field, Pattani Basin, Allan diagram, Shale Gouge Ratio (SGR).

ACKNOWLEDGEMENTS

This report has been achieved because of the help, suggestions and supporting from many people. Firstly, I would like to sincerely thank my project advisor, Dr. Kruawun Jankeaw for all of her suggestions and dealing with any obstructions during my research. I would like to kindly thanks Mubadala Petroleum (Thailand) Limited. for giving me the opportunity to do this senior project and for providing of company data and equipment to and also for giving me new knowledge and experience. I am grateful and indebted to my co-advisor; Ms. Angela Echanove and Mr. Rahmat Utono for sharing expertise, sincere and valuable guidance, and encouragement extended to me.

Special acknowledgements to Mr. Tianpan Ampaiwan for encouragement and reviewing manuscripts and general help throughout this research. Additionally, special thanks to Ms. Thirada Kensakoo for her assistance, invaluable suggestions, and teaching software use.

I would like to deeply thank Department of Geology, Faculty of Science Chulalongkorn University for giving me numerous fundamental knowledge and suggestion.

Finally, this senior project cannot be completed without the help and encouragement of my family who patiently provided both moral and physical support and my friends in Geo'56 for assistance and cheerfulness and I appreciate all of the support from the others that have not been mentioned too.

CONTENTS

Page

LIST OF FIGURES

LIST OF TABLES

CHAPTER 1

INTRODUCTION

1.1 Rationale

In petroleum exploration, faults play an important role in creating hydrocarbon traps that can control the distribution of hydrocarbon. In addition, fault zones can act as either barrier or preferential flow paths to fluid (Knipe et al., 1997; Bense et al., 2003). In fact, the problems that happen when predicting reservoir distribution are difficult because of multiple faults, complex reservoir and seal geometry, and the opportunity of across-fault leakage and migration (Williamson, 1992). The study of sealing mechanism and the evaluation of effective fault sealing are important to predict the petroleum reservoir distribution. Furthermore, these can help us to understand the processes that contribute to fault seals and also to analyse the cause of leakage in the fault zone. Fault seal study has many methodologies to investigate the potential sealing on fault surface. For example, Allan diagram (fault plane map) was used to predict trapped area in faulted closure. Moreover, Shale Gouge Ratio (SGR) calculation was used to identify the potential of hydrocarbon seal in zone of shear smear on fault surface.

The Jasmine Field is located on the Northern part of Pattani Basin, Gulf of Thailand (Figure 1-1). The structural closures and play types in the area are influenced by several major structural trends. The trap styles are both structural and stratigraphic traps associated with faults. In addition, the hydrocarbon accumulation in the field was generally trapped by fault sealing mechanism, whereas some reservoir horizons have differences in hydrocarbon contacts on either side of the fault. Therefore, fault seal assessment is a crucial approach to analyse and find an answer of how the fault can be sealed. Besides, the methodology and the result from this research can be applied to predict the fault seal capacity in the other areas of similar structure and lithology and also to predict the potential accumulation areas in the future.

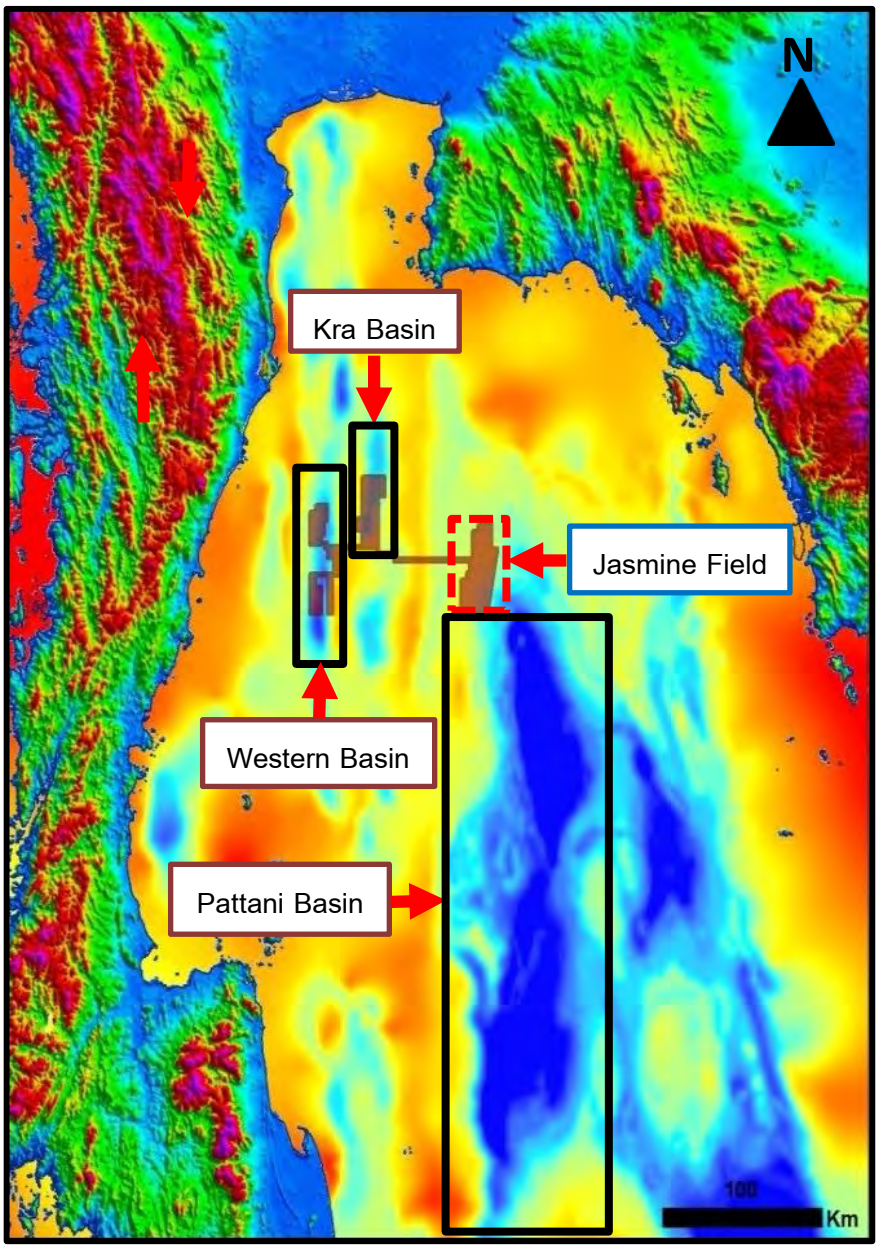

Figure 1-1 Location of the Jasmine Field located in the Northern part of Pattani Basin, Gulf of Thailand (Mubadala Petroleum (Thailand) Limited).

1.2 Study Area

The study area is Jasmine A which is a part of Jasmine Field located in Block B5/27, Northern part of the Pattani Basin in Gulf of Thailand. This area lies between latitude 11°17’43” N to 11°19’ 30” N and longitude 101°12’40” E to 101°14’18” E. Approximate area is 10 square kilometers (Figure 1-2).

1.3 Objectives

1. To test if Allan diagram (fault plane map) is efficient in evaluating fault sealing for hydrocarbon accumulation.

2. To identify potential sealing of fault by using SGR.

1.4 Methodology

1. Study previous works of fault seal analysis and literature review on regional geology and petroleum system of Jasmine Field, Northern part of the Pattani Basin, Gulf of Thailand.

2. Collect and prepare data (e.g. well data, seismic data and cutting samples) for identifying the possibility of fault sealing.

3. Construct depth structure map, net sand (isopach) map and Allan diagram along the faults in Jasmine A area.

4. Calculate SGR using the triangle diagram and measure across-fault pressure difference by using pore pressure profile.

5. Identify the mineral composition of cutting samples using X-ray diffactometer (XRD) technique.

6. Establish the calibration diagram of SGR against across-fault pressure difference.

7. Analyse and interpret results to explain the main controlling factor for hydrocarbon accumulation and hydrocarbon column heights.

8. Discuss and conclude the project study.

9. Make a research report and presentation.

1.5 Scope of work

Mineral composition of cutting samples are identified with XRD technique. Seismic data is used to interpret geological structure and to construct depth structure map, net sand map as well as the model cross section of Allan diagram. Well data is used to calculate SGR and across-fault pressure difference and also pore pressure gradient of the Jasmine Field, Northern part of the Pattani Basin in the Gulf of Thailand.

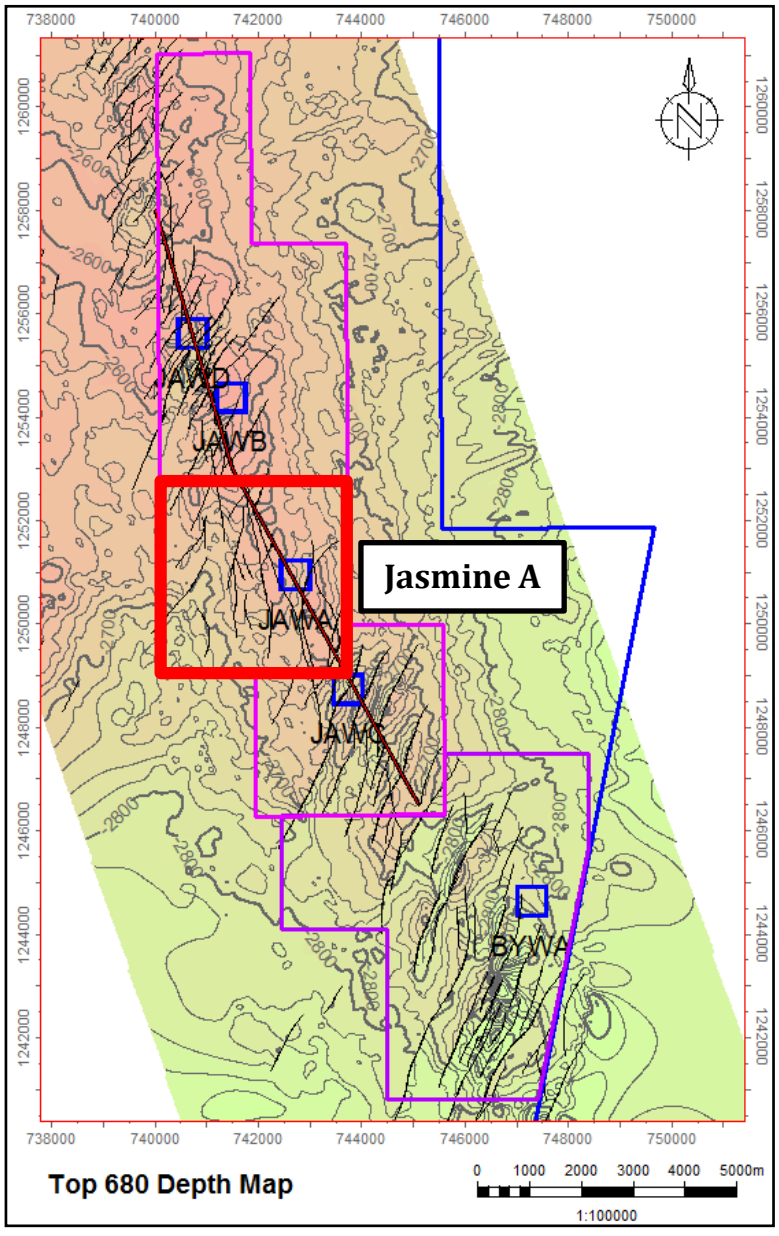

Figure 1-2 Top 680 horizon depth structure map shows the location of the Jasmine Field and the red rectangle represents the study area (Jasmine A).

1.6 Previous works

There are many previous works for evaluating or predicting the possibility of fault sealing by juxtaposition. This section divided previous works into 2 parts; model cross section of Allan diagram showing an overview of potential leak and seal points on the fault plane and fault seal mechanism identified by SGR in the sand-to-sand juxtaposition area.

1.6.1 Model cross section of Allan diagram

Allan (1989) presented a model, namely Allan diagram or fault plane section, that relates faults to migration and entrapment. Allan diagram has been used in evaluating fault seal distributions and illustrated stratigraphic geometries of horizon/fault plane intersections. The model is based on the following simple assumptions: (1) a fault itself has no sealing properties, (2) a fault is not an open conduit and (3) the trapping and migration relationships at a fault depend upon the fault juxtaposed stratigraphy. Moreover, this model can be used to explain the migration pathway on the fault plane.

Tang-on (2014) studied the fault seal analysis in Arthit Field, North Malay Basin, Gulf of Thailand by using juxtaposition models (Allan diagram) which display the sophisticated sand/shale layers and investigate the area of fault seal and fault leak. There are four cases of results that illustrated investigations of juxtaposition models; case 1: Sand-to-shale juxtaposition area which can trap gas without any leakage zone, case 2: Sand-to-shale juxtaposition area which is the area of the laterally connectivity of wet sand, case 3 and 4 are the sand-to-sand juxtaposition which can trap gas and water, respectively. However, both of case rarely presents in Arthit field.

1.6.2 Fault seal mechanism identified by SGR in the sand-to-sand juxtaposition area

Seals are any lithology that form a barrier to subsurface fluid flow. They are considered as membrane seals or hydraulic seals, depending on their likely failure mode (Watts, 1987). The dominant control on failure of membrane seals is the capillary entry pressure of the seal rock; that is, the pressure required for hydrocarbons to enter the largest interconnected pore throat of the seal. When the entry pressure has to exceed the strength of the rock in order to breach the seal, the seal is considered a hydraulic seal.

Vavra et al. (1992) presented that the seal capacity in holding back hydrocarbons which is controlled by the size of the largest interconnected continuous pore throats and the relative densities of the hydrocarbon (oil or gas) and formation water.

Knipe (1997) presented the juxtaposition diagram (triangle diagram) for analysing fault juxtaposition and sealing. The triangle diagram is used to calculate the SGR value which is based on the interaction of lithology and fault displacement to control juxtapositions and fault seal types.

Yielding et al. (1997) presented the factors that control the likelihood of clay/shale smearing as follows: (1) thicker source beds can produce thicker clay smears, (2) shear-type smears decrease in thickness with distance from the source layer, (3) abrasion-type smears decrease in thickness with increasing throw, and (4) multiple source beds can give a combined continuous smear. These relationships can imply that a quantitative approach can be applied to predict clay smear in fault zone.

Fisher and Knipe (1998) studied the relationship between SGR and outcrop. They classified fault rock and fault seal types based on their composition. In addition, the clay content is defined by SGR at the time of deformation. The SGR can be considered as a predictor of fault-rock types for simple fault zone.

Gibson (1998) studied and measured the permeability of fault gouge sample in siliciclastic strata of the Columbus basin. The results can be concluded that the permeability of fault gouge is dominated by the phillosilicate content; when phillosilicate content increase results the permeability of the fault gouge is low.

Koednok (2002) studied the influence of clay and shear smear in fault zone on the potential sealing of hydrocarbon in Block B8/32, Pattani Basin, Gulf of Thailand. The SGR of fault in the Benchamas-A is ranges of 40-86% which can seal hydrocarbon on the fault plane in the sand-to-sand juxtaposition area.

Yielding et al. (2002) suggested that the SGR value in ranges of 15-20% represented a threshold value between non-sealing and sealing faults in the Oseberg Syd Field. The values of SGR generally indicate the potential to hold back higher pressures (trap greater hydrocarbon columns) at sand-to-sand juxtapositions.

Bretan et al. (2003) suggested that the calibration diagram of the SGR against across-fault pressure difference can estimate the maximum height of a hydrocarbon column that can be supported by the fault. Leakage of hydrocarbons across-fault occurs when the buoyancy pressure exceeds the capillary entry pressure of the fault and is not confined to the crest of the structure or even to where the SGR value is the lowest.

1.7 Expected results

1. Model cross section of Allan diagram showing areas with self juxtaposition and juxtaposition with different units.

2. SGR that is effective for sealing of hydrocarbon in the study area.

CHAPTER 2

GENERAL GEOLOGY

2.1 Regional Geology

The Gulf of Thailand is composed of several Tertiary basins which are generally formed as parallel N-S trending rift basins. They formed in response to the extensional setting caused by regional tectonic activity of the northward collision of the Indian and Eurasian plates in the early Tertiary (Polachan et al., 1991). Gulf of Thailand is seperated by the N-S trending Ko Kra Ridge into two main parts; western and eastern parts. The western part contains ten basins of various sizes; Sakhon, Paknam, Hua Hin, Prachuap, Northwestern, Western, Kra, Chumporn, Nakhon, and Songkhla. The eastern part comprises of two major basins, namely Pattani and Malay Basins (Charusiri et al., 1997).

The Pattani Basin is the largest offshore Cenozoic basin, and is the most productive for hydrocarbon-bearing traps in Gulf of Thailand (Jardine, 1997). It is approximately 270 km in length and 100 km wide (Watcharanantakul and Morley, 2000). The basin is attributed by a series of elongate N-S trending rifts and mainly dominated by graben and half-graben structures controlled with the NW-SE and NE-SW directions of strike-slip faults. There are two main models for the basin development; pull-apart basin established by the strike-slip movements of the NW-SE trending Three Pagodas fault zone and the NE-SW trending Ranong-Khlong Marui fault zone (Polachan et al., 1991) (Figure 2-1a). In the other model, most of the rift basins in Tertiary age are primarily extensional but complicated by inversion and strike-slip reactivation (Morley, 2001) (Figure 2-1b). Watcharanantakul and Morley (2000) suggested that during late Oligocene-early Miocene, strike-slip faults in the Gulf of Thailand were inactive and that the extension is due to E-W extensional stresses generated by subduction rollback, superimposed on the region of escape

tectonics. The Pattani Basin has a relatively high geothermal gradient range of between 36° and 63° C/km and heat flow between 80-105 m.W/w^2 (Bustin and Chonchawalit, 1995).

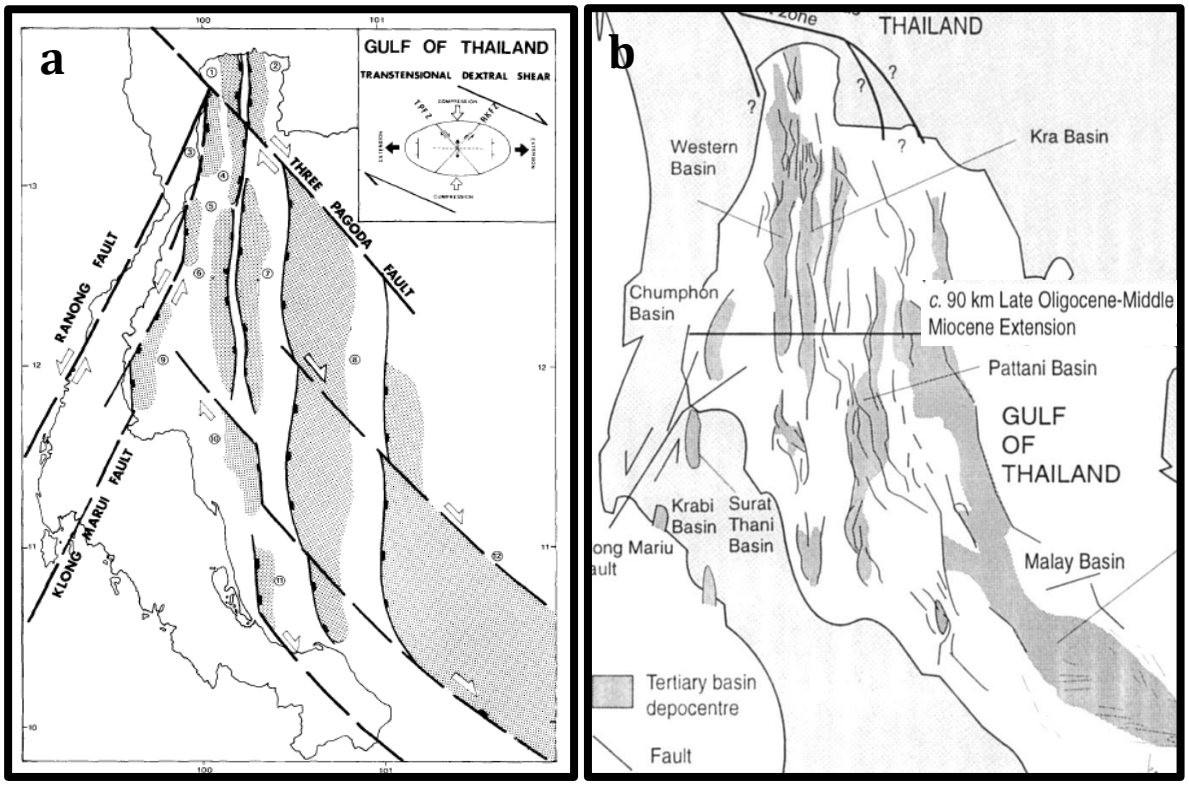

Figure 2-1 (a) Structural map of the Gulf of Thailand, showing relationship between conjugate strike-slip faults and the development of N-S trending pull-apart basins (after Polachan, 1991). (b) A model for the evolution of the rift basins in the Gulf of Thailand that strike-slip faults were inactive and extension due to E-W extensional stresses generated by subduction rollback, superimposed on the region of escape tectonics (Morley, 2001).

2.2 Structural Framework

The Jasmine Field is located on the northwestern flank of the Pattani Basin. It was formed in NW-SE direction and is dissected by numerous N-S trending normal faults. The structure in the area consists of major fault trends; NNW to SSE and NE to SW directions formed by a series of normal fault blocks that split a south-southeast plunging anticline. Many of the normal faults are arranged in en-echelon pattern that

is a component of right-lateral strike slip motion which occurred along the Jasmine Field trend. The structural history of the Jasmine area is typically that of the Pattani Basin which comprises syn-rift and post-rift sequences. In addition, the structural evolution of the basin can be subdivided into seven main stages (Jardine, 1997):

1). Pre-rift folding and uplift of pre-Tertiary accreted basement terranes from the Cretaceous to the Eocene;

2). Initial rifting and creation of localized sub-basins (half-grabens) from Late Eocene to Late Oligocene time;

3). Structural inversion and erosion at the end of the Oligocene;

4). Rifting and basin formation in the Lower Miocene;

5). Post-rift collapse and basin subsidence in the Middle Miocene;

6). Widespread erosion in Latest-Middle to Early-Upper Miocene time; and

7). Continued basin subsidence from the Upper Miocene to the present.

Jardine (1997) suggested that during the main rifting and basin formation phase in the early and middle Miocene, the Pattani trough subsided relatively rapidly. "Accommodation" graben systems consisting of a series of opposing normal faults developed in response to the rapid extension and deepening. Faults are activated through time while the deposition of sediments which eroded from the high structure, still continue. In Oligocene to early Miocene time, the syn-rift section accompanied rifting and extension, with episodic block faulting and rapid subsidence. The basin morphology is controlled by a series of major en-echelon extentional faults. The largest syn-rift faults have displacements up to a few kilometers (Morley, 2004). In the post-rift section, conjugate normal faults system from a network of fractures that extend from the basement ran into upper Miocene units (Kornsawan and Morley, 2002; Morley et al., 2004).

2.3 Sequence stratigraphy

The stratigraphy of the Tertiary basins in the Gulf of Thailand is dominantly non-marine and consists of thick successions of Oligocene and Miocene fluvial and lacustrine strata that were deposited before marine inundation in the latest Miocene to Pliocene. Several regional stratigraphic schemes have been derived for the Tertiary succession (Jardine, 1997). Mubadala Petroleum divides the Gulf of Thailand Tertiary succession into 8 sequences whose boundaries generally correspond to tectono-stratigraphic events (Figure 2-2). These are designated as sequence 10 (S10) to sequence 80 (S80) from oldest to youngest, respectively. In the Jasmine Field, the stratigraphic sequences are the sequence deposited during the middle-late Miocene age (Figure 2-3); sequence 50 to 70 (S50-S70). The brief summary of these sequences are concluded below (as interpreted by Mubadala Petroleum; 2008) and shown in Figure 2-3.

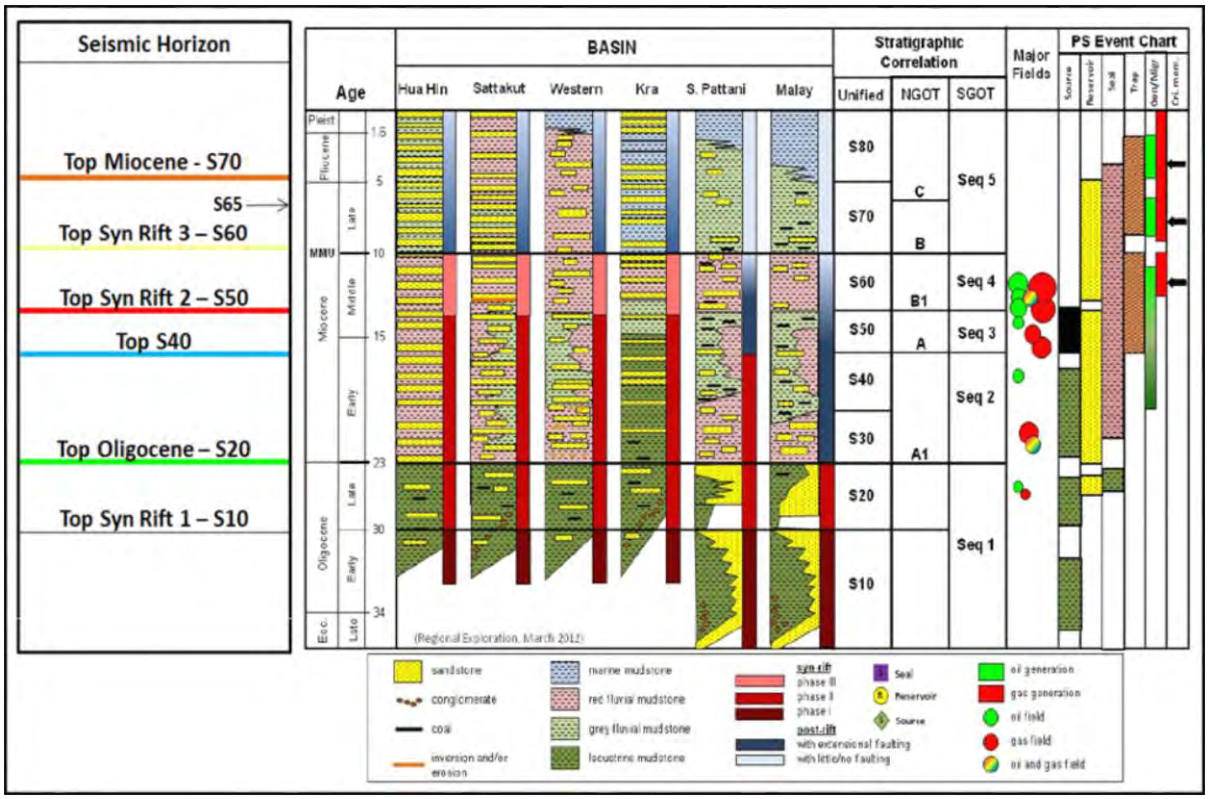

Figure 2-2 Gulf of Thailand unified stratigraphy (Mubadala Petroleum, 2008).

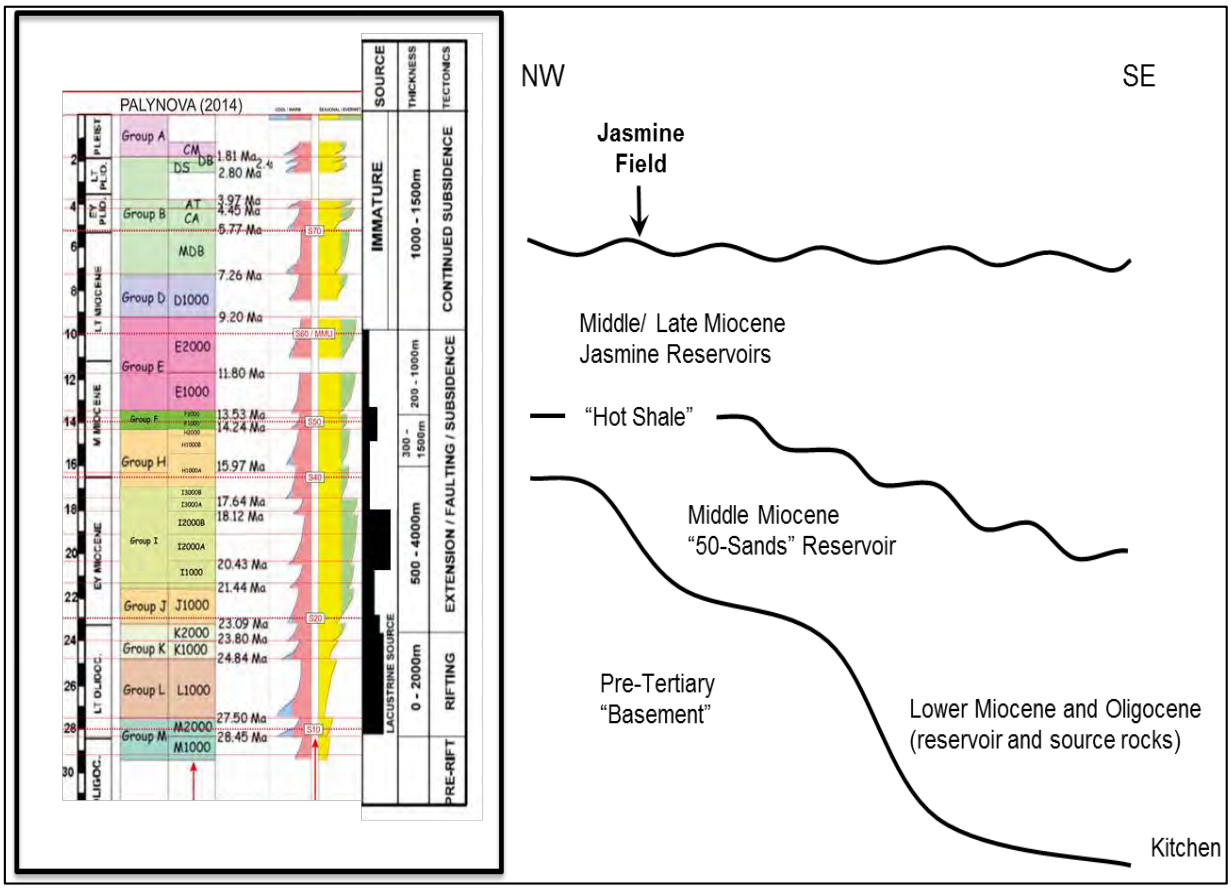

Figure 2-3 Geologic and stratigraphic setting in Jasmine Field (Mubadala Petroleum, 2008).

2.3.1 Pre-Tertiary Basement

Pre-Tertiary Basement is the pre-rift tectonism associated with mainly marine carbonates, usually crystallized Permian limestone (Ratburi Formation) with occasional mudstone that infilled karsts and fractures. Lithologies are described as hard, compact, shales/phylites and sandstones orthoquartzite. Moreover, the section is characterized as low grade metamorphic. The pre-Tertiary sediments are truncated by a major regional unconformity (Pre-Tertiary Unconformity or PTU).

2.3.2 Syn-rift sequence (Sequences 10 to 60)

Sequence 10 (S10) corresponds to early Oligocene and early syn-rift deposits that are commonly dominated by lacustrine shale and deltaic sandstones with subordinate proportions of lacustrine carbonates and coals, whereas late Oligocene syn-rift strata, again commonly dominated by lacustrine shale, comprise S20. S30 and S40 are early Miocene late syn-rift to early post-rift sequences that are primarily fluvial, although lacustrine intervals are common in some basins, especially in S40, plus there are minor local marine incursions. The latest early Miocene to end middle Miocene S50 and S60 are the latest syn-rift to post-rift fluvial strata with minor lacustrine and marine intervals.

2.3.3 Hot Shale sequence

The ‘Hot Shale” sequence is the late Oligocene or the earliest Miocene in age which is influenced by lacustrine environment. Local depositional environments could vary rapidly laterally, but fan deltas appear to dominate the early graben fill in the Jasmine area. This unit is thin in the area, from approximately 120 ft in the south to less than 50 ft in the north. Occasionally, interbeded within the shale are thin fine-grained sands, which become more common northwards during the late graben fill section. The regional highstand led to the development of laterally extensive swampy lagoonal conditions. The section is subdivided into two units; the upper and the lower units. The upper unit is characterized as an lacustrine plain, a low sand/shale ratio and thin individual sand bodies that are vertically discrete bodies. For the lower units, it is characterized as a fan delta, a very high sand/shale ratio and moderately thick to massive individual sand bodies separated by thin shale such that sands are probably vertically discrete.

2.3.4 Post-rift sequence (Sequences 70 to 80)

Sequence 70 (S70) and sequence 80 (S80) are post-rift units; S70 is of the late Miocene age and is typically fluvial but becomes marine in some basins whilst the Pliocene S80 generally is fluvial in the North and progressively marine southward. These sequences represent a relatively thin transgressive sequence of variable lower coastal plain mangrove facies of Pliocene and probably late Miocene age. Open marine inner neritic conditions were finally established as the topmost of section which are clay dominated with interbeded sands.

CHAPTER 3

METHODOLOGY

The methodologies in this research are based on previous studies such as Allan diagram, Yielding's quantitative fault seal prediction and estimating hydrocarbon column heights by using shale gouge ratio calibration. These methods were applied in this study to create the appropriated approaches for analyzing and evaluating the fault sealing in study area. The data acquisition and the methodology are described as follows.

3.1 Data Acquisition

All data in this study are provided by Mubadala Petroleum (Thailand) Limited. The data are composed of well log data, seismic data, cutting samples and internal company reports. The data can be concluded as below:

1) Well report of 7 wells (JA-02, JA-03, JA-05, JA-16, JA-23, JA-27 and DL-4).
2) Wireline log of 7 wells (JA-02, JA-03, JA-05, JA-16, JA-23, JA-27 and DL-4) comprise gamma ray, resistivity and neutron-density logs.
3) Top depth structure map of 6 horizons (460, 400, 330, 250, 200 and 140).
4) Cutting samples of 2 wells (JA-23 and JA-27) total 11 samples.

In this research, mineral composition of cutting samples are identified with XRD technique. Seismic data is used to construct depth structure map, net sand map as well as the model cross section of Allan diagram and also to interpret structure and reservoir geometry. Well data is used to calculate SGR and across-fault pressure difference and also pore pressure gradient. In addition, this data is used to identify lithology and fluids as well. The steps of work are shown in the workflow diagram (Figure 3-1). Finally, all results are used to evaluate fault seal capacity and to estimate the maximum height of a hydrocarbon column supported by the fault.

WORKFLOW DIAGRAM

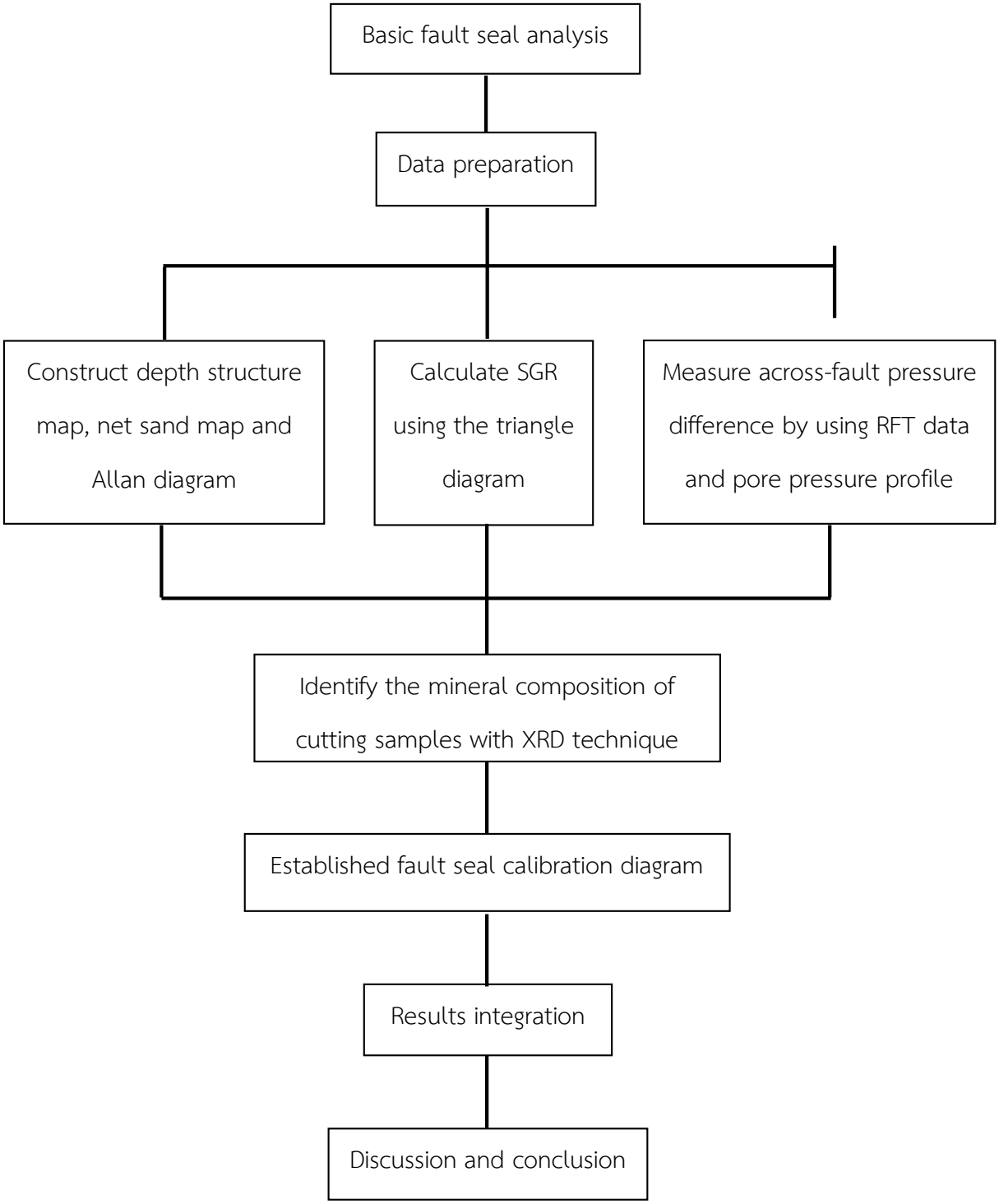

Figure 3-1 Flow chart of the method used in this study.

3.2 Methodology

Triangle juxtaposition diagram worksheet (Microsoft Excel), Petrel and Pressure Explorer software are the available materials which are used to analyse the results in this study. However, there are some processes which are modified to best fit with the available data. The typical procedure for this study is described as follows:

1. Study previous works of fault seal analysis and literature review on regional geology and petroleum system of Jasmine Field, Northern part of the Pattani Basin, Gulf of Thailand.

2. Collect and prepare data (e.g. well data, seismic data and cutting samples) for identifying the possibility of fault sealing.

3. Construct depth structure map, net sand map and Allan diagram along the faults in Jasmine A area.

4. Calculate SGR using the triangle diagram and measure across-fault pressure difference by using pore pressure profile.

5. Identify the mineral composition of cutting samples using XRD technique.

6. Establish the calibration diagram of SGR against across-fault pressure difference.

7. Analyse and interpret results to explain the main controlling factor for hydrocarbon accumulation and hydrocarbon column heights.

8. Discuss and conclude the project study.

9. Make a research report and presentation.

3.3 Conceptual approach

3.3.1 Basic fault seal analysis concept

All of the research methodologies referenced to the methodology of previously published studies such as SGR calculation using the triangle diagram published by Yielding et al. (1997) and Freeman et al. (1998). However, the processes in this study have to change some steps to fit with the available data of the study area. The fault seal study is based on the following simple assumptions:

1. Both the hanging wall and the footwall side have the same stratigraphy and where there are non-reservoir (shale) juxtaposed against reservoirs (sands), those juxtaposed areas have sealing potential (Allan, 1989).
2. The fault-gouge composition is dominated by the bulk composition of the wall rocks that have slipped past that point on the fault (Yielding et al. 1998).
3. All pressure plotted against depth, should lie on a same straight line and each layer in each compartment, there are no pressure barriers, that is, all the changes in pressure occur across the faults (Yielding, 1999).

3.3.2 Data preparation

Types of data for evaluating the possibility of sealing faults in this study are divided into two categories; well data and drill cuttings. These data are described as below.

3.3.2.1 Well data

For analyzing fault sealing tendency in this research, the well data consists of:

1. True vertical depth (TVD)
2. Volume of clay (Vcl.) and pore pressure data
3. Fluids and lithology
4. Well logs (gamma ray, resistivity and neutron-density logs)

In this research, the well logs are used to construct the model of stratigraphic layers by correlating the horizon from well to well and generate the section of stratigraphic layers. These stratigraphic layers can give an idea for creating stratigraphic continuity on the fault plane. Moreover, the well log correlation is important data to guide constructing other modules such as structure map, net sand map, SGR calculation and measuring across-fault pressure difference. The well log correlation are shown in Figure 3-2

3.3.2.2 Cutting samples

The cutting samples used in this study were selected from the well which represent each fault blocks in the study area. These samples were collected at the depth interval identified from 2D seismic line indicating thick and continuous shale layers. The depth interval of samples are shown in Table 3-1

Table 3-1 Depth interval of 11 samples from 2 wells; JA-23 and JA-27 which were collected at 60 ft and 30 ft interval, respectively.

Samples	Depth interval (ft)	Samples	Depth interval (ft)
JA-23-1	5500-5560	JA-27-1	5020-5050
JA-23-2	5620-5680	JA-27-2	5230-5260
JA-23-3	5860-5920	JA-27-3	5380-5410
JA-23-4	6040-6100	JA-27-4	5530-5560
JA-23-5	6220-6280	JA-27-5	5710-5740
		JA-27-6	6040-6070

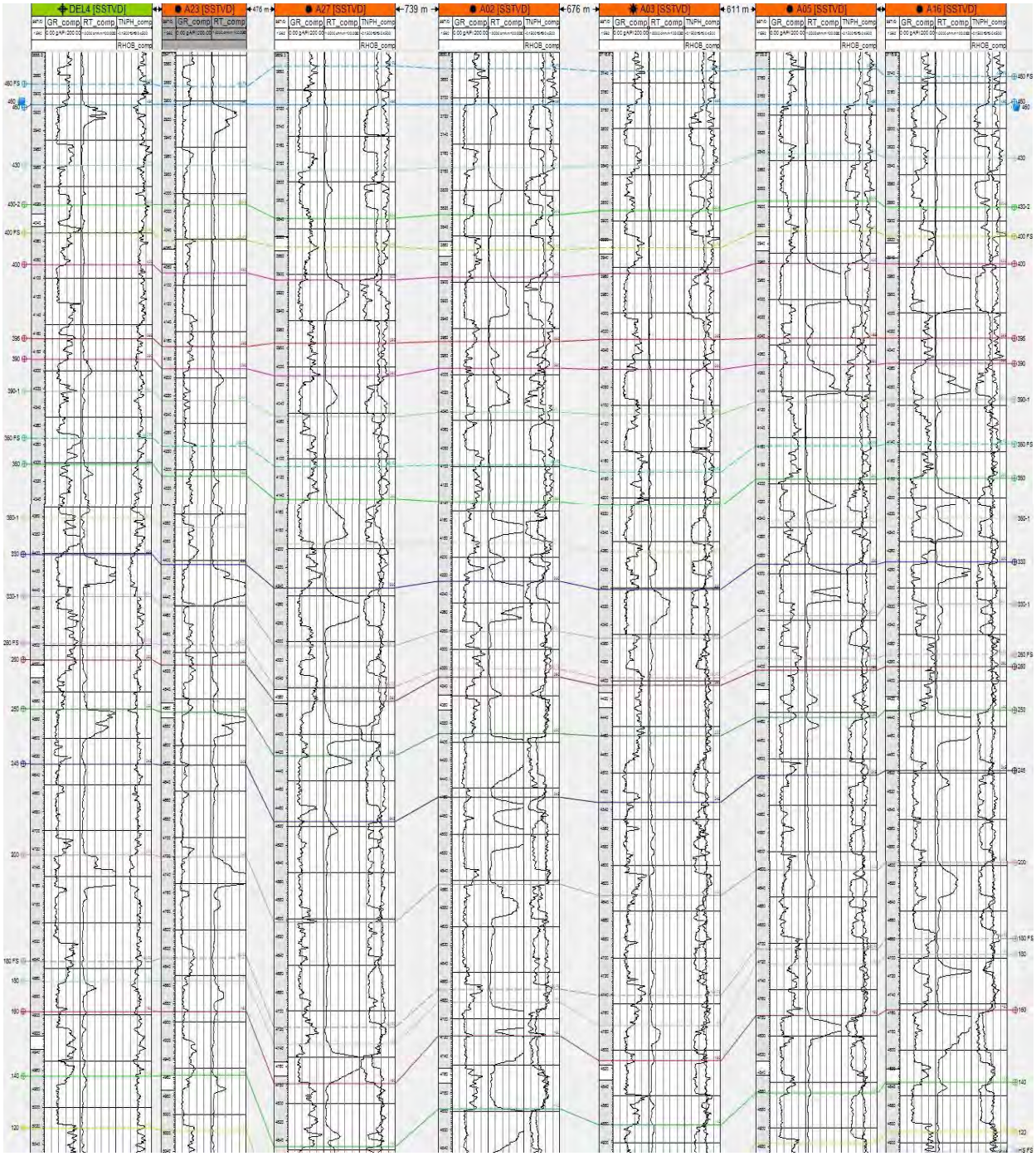

Figure 3-2 Well log correlation in Jasmine A area which correlates from west to east. Gamma-ray log is on a left side, whereas resistivity log and neutron-density log are at the right side in each well.

3.3.3 Construct top depth structure map and net sand map

The depth structure map and the net sand map are constructed to have understanding of the subsurface topography across-fault, sand distribution and sand thickness of the top sand horizon for creating the model cross section of Allan diagram. Furthermore, the depth structure map can be applied to investigate the area of hydrocarbon accumulation and the migration pathway in each main reservoirs.

3.3.4 Construct Allan diagram

The Allan diagram (Figure 3-3) displays an overview of lithological and fluid juxtaposition across a fault. The construction of Allan diagram is based on an encountered wells in which the study area was penetrated by 29 wells and the location of these wells are close to fault. These wells provided adequate data for generating the Allan diagram along faults. Additionally, the Allan diagram analysis is an approach to identify fault traps and probable high permeability pathways along fault.

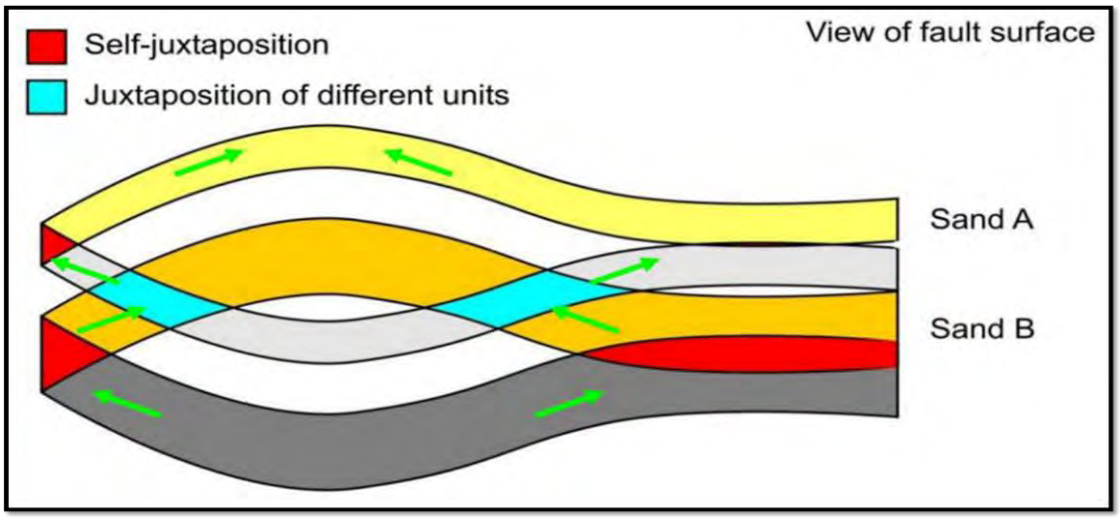

Figure 3-3 Example of the Allan diagram shows juxtaposition relationships of different stratigraphic layers. Colors represent different layers with different reservoir quality and different contacts across the fault (after Allan, 1989).

3.3.5 SGR calculation

SGR is one of algorithm for predicting clay smear which can form an effective seal along the fault zone. This algorithm is used to estimate the composition of subsurface fault zone which is the proportion of clay/shale material that might be entrained in the fault zone. Fundamentally, the SGR can consider from the percentage of shale or clay in the slipped interval (throw) illustrated in Figure 3-4. The SGR based on calculated clay volume, bed thickness and throw with the equation as show below:

$$\text{SGR (\%)} = \frac{\Sigma[(\text{zone clay fraction, Vcl.}) \times (\text{zone thickness, } \Delta z)]}{\text{Fault throw, t}} \times 100\%$$

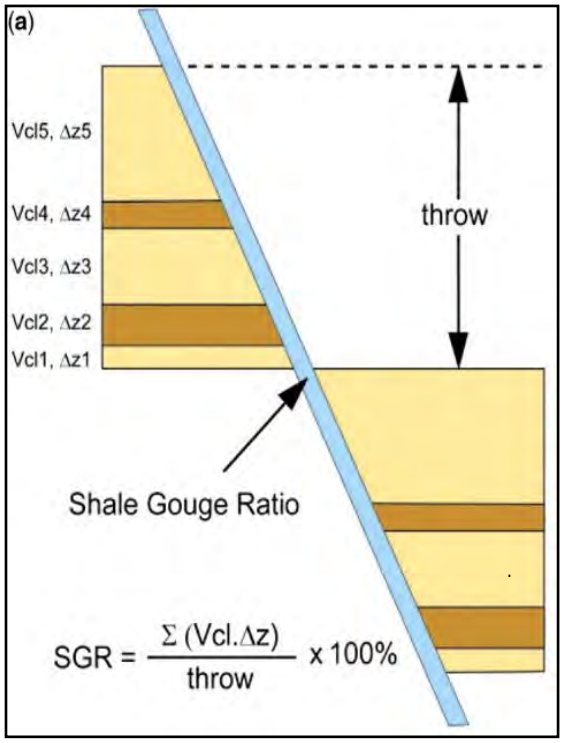

Where:

Vcl.= volume of clay is in individual thickness.

Δz = individual clay bed thickness in slipped interval.

t = vertical slipped thickness (slipped interval) that considered at any point on fault

Figure 3-4 The definition of SGR which reflects the proportion of the sealing lithology in the rock interval that has slipped past a given point on the fault (after Yielding et al., 1997).

There is an alternative computation, widely used in the petroleum industry that is also referred to by the triangle diagram shown in Figure 3-5. This diagram is a quick-look prediction of juxtaposition method which requires the input of clay/shale content of the faulted section.

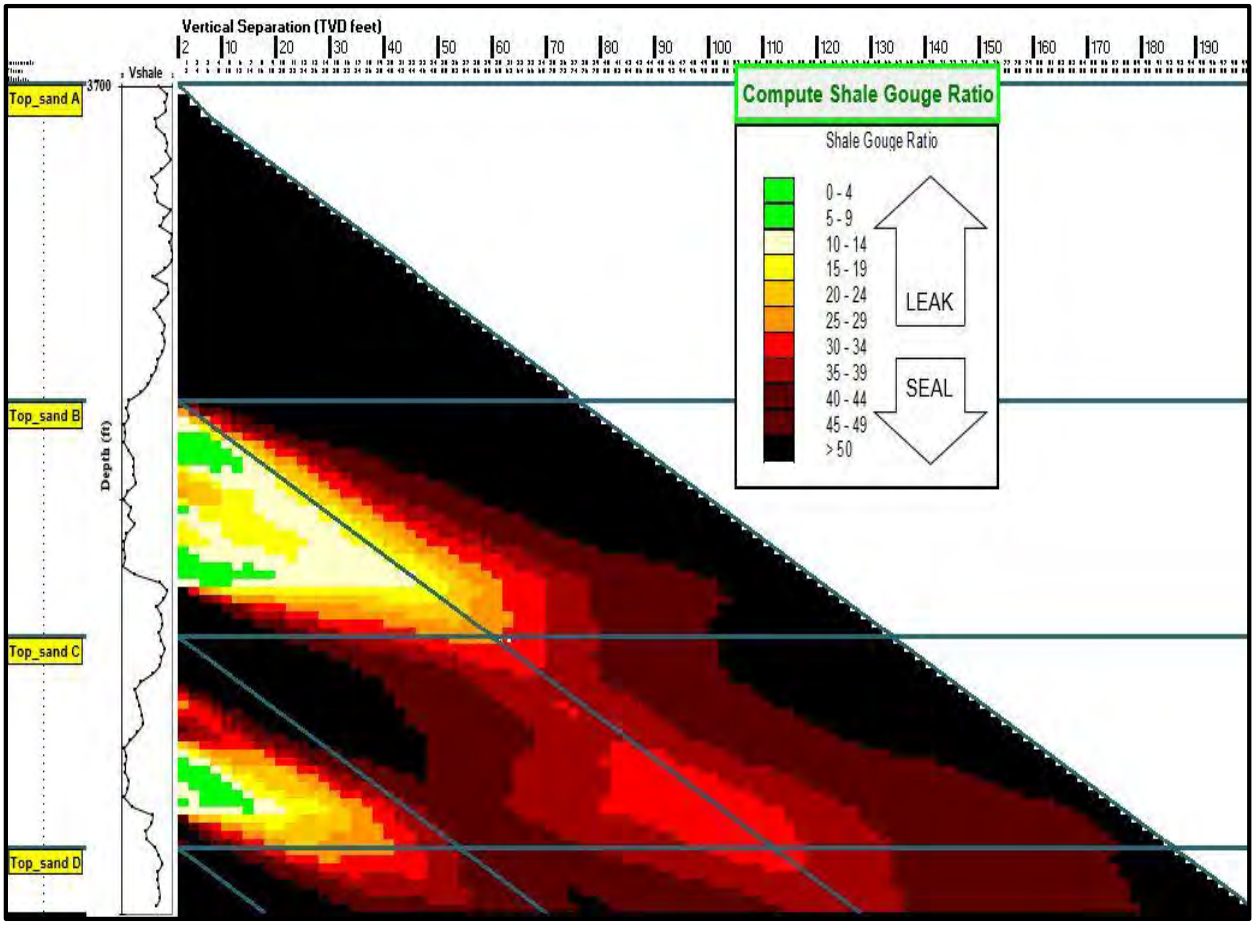

Figure 3-5 Triangle diagram illustrates the SGR calculation at a given point on a fault surface for explicit shale beds. It was defined in publications by Yielding et al. (1997) and Freeman et al. (1998).

3.3.6 Across-fault pressure difference measurement

Across-fault pressure difference is measured from the pressure data at the same depth. That data will be shown in the pressure profile which is plotted by the Repeat Formation Test (RFT) data of the well in a fault-bound block. The pore pressure profile (Figure 3-6) will display the pressure and depth relationship as a linear trend along each reservoir zone from the well to the fault using the appropriate fluid densities.

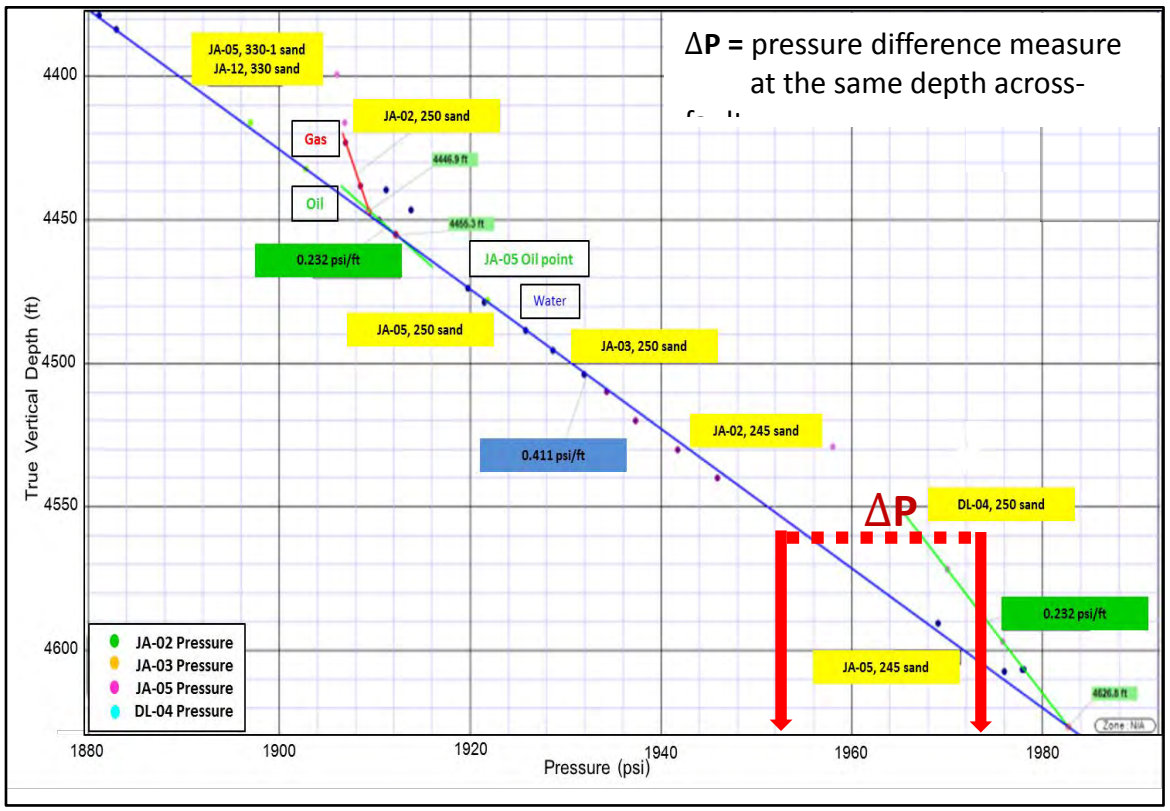

Figure 3-6 Example of the pore pressure profile illustrates the across-fault pressure difference measurement of the different fluid types in sand-to-sand reservoir juxtaposition. The red, green and blue lines represent the gas, oil and water gradient of the 250 reservoir sand horizon and the green, orange, pink and blue dots represent the RFT data of wells in the Jasmine A area.

The pore pressure data can identify the fluid type and interpret the physical properties of fluid in each reservoir zone such as fluid density and the depth of fluid contact. Type of fluid gradient is represented by the value of 1/slope in the pressure depth diagram and depth of difference fluid contact in the system is represented by the intersection point between two slope lines. Moreover, the continuous RFT data on a same straight line between wells represents reservoir continuity. The fluid properties such as specific gravity, API gravity and hydrostatic pressure gradient are shown in Table 3-2.

Table 3-2 Relationships among specific gravity, API gravity, hydrostatic pressure gradient (psi/ft), and total dissolved solids for brines (Dahlberg, 1994).

Specific gravity	**API gravity**	**Hydrostatic pressure gradient**	**Total solids (ppm)**
2.50	-7.5	1.083	210,000
2.00	-5.2	0.866	175,800
1.50	-2.7	0.650	143,500
1.25	3.0	0.541	69,500
1.20	10.0	0.520	0
1.14 (brines and heavy oils)	17.0	0.494	
1.12	25.0	0.485	
1.10	35.0	0.476	
1.05	45.0	0.455	
1 (fresh water)	60.0	0.433	
0.95		0.411	
0.90		0.390	
0.85 (light oil)		0.368	
0.80		0.346	
0.70		0.303	
0.55		0.238	
0.50 0.216		0.216	
0.40 (gas)		0.130	
0.20		0.086	
0.15		0.065	
0.10		0.043	

3.3.7 Identifying mineral composition from cutting samples

The cutting samples are used to identify mineral composition and study clay mineral assemblage that may affect hydrocarbon accumulation in reservoir sand horizon. For this process, samples were selected with binocular microscope after that the XRD technique was used in identifying mineral composition and quantifying the proportions of different minerals. The algorithm of XRD analysis is the detection of peak positions using the intensity and Q-spacing of minerals. The results is displayed with the peak matching as shown as an example in Figure 3-7.

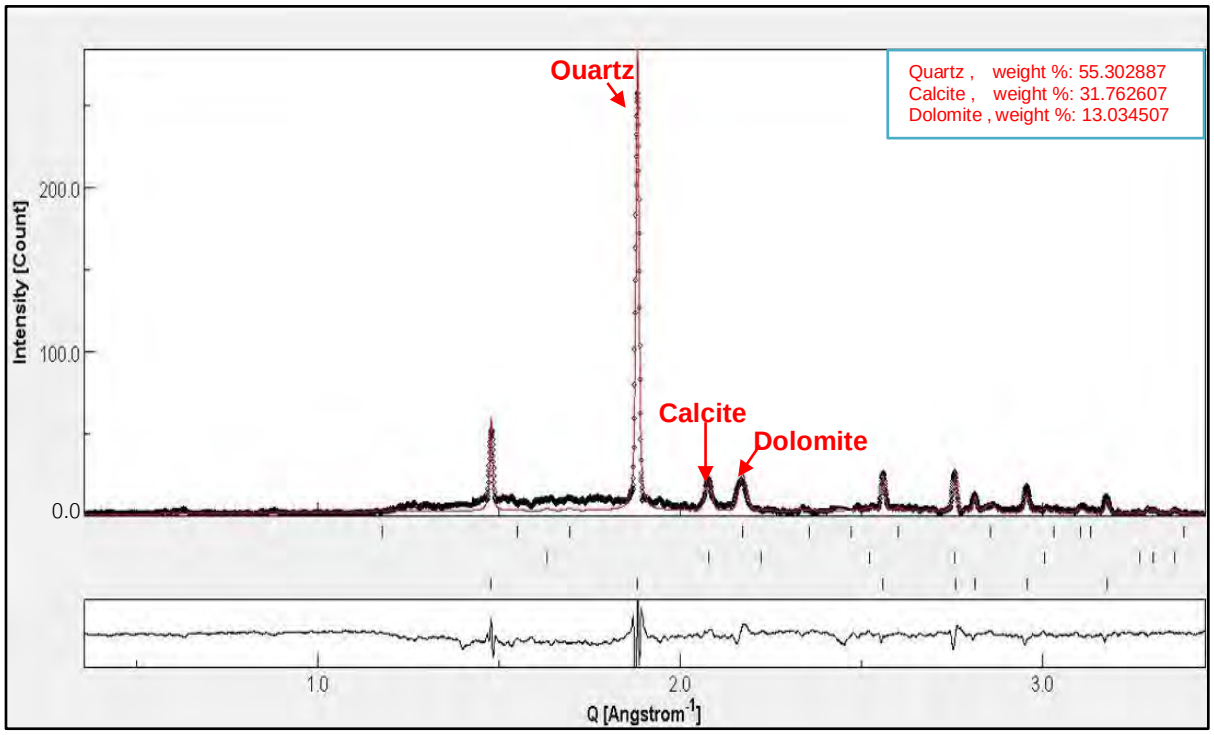

Figure 3-7 Example of XRD analysis of the cutting sample from well JA-23 showing the peak position, intensity and Q-spacing.

3.3.8 Establish the fault seal calibration diagram

The fault seal calibration diagrams are established to estimate the hydrocarbon column height in the other areas that have similar geological structure and depositional environment. The diagram is the SGR calibration with the across-fault pressure difference in the area of sand-to-sand reservoir juxtaposition as shown in Figure 3-8. Hydrocarbons can leak across a fault when the buoyancy pressure exceeds the capillary entry pressure of the fault and is not confined to the crest of the structure or even to where the SGR value is the lowest (Bretan et al. 2003).

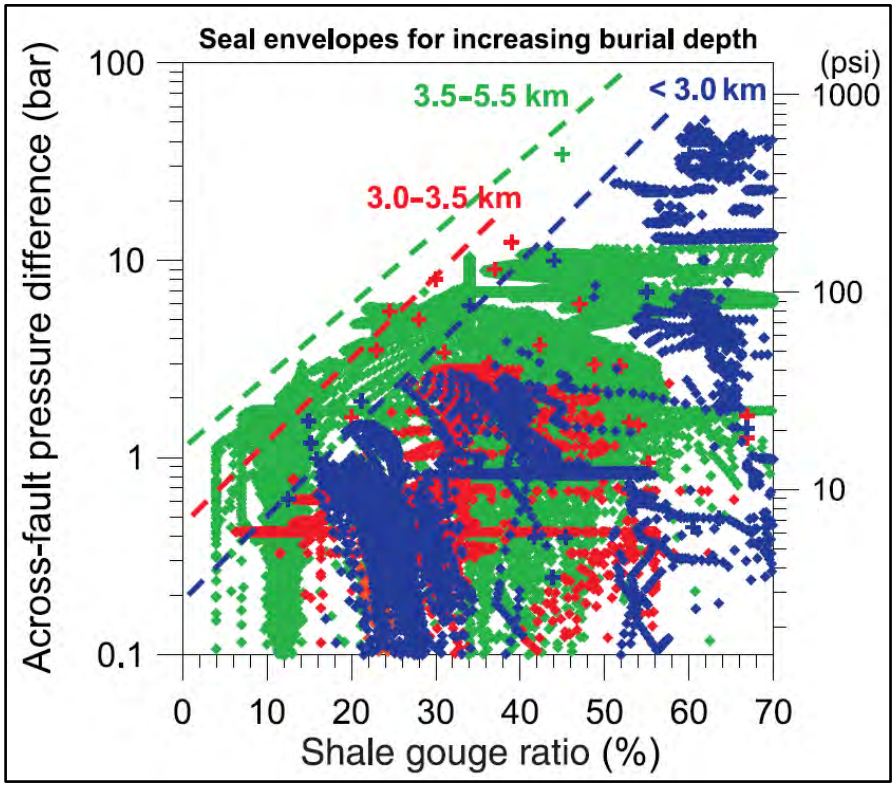

Figure 3-8 Example of the calibration plot of SGR against across-fault pressure differences for sand-to-sand reservoir juxtapositions from basins. The red, green and blue dash lines represent the burial depth of basins worldwide and the red, green and blue dots represent a variety fault data from basins worldwide (Yielding 2002; Bretan et al., 2003).

CHAPTER 4

RESULTS AND INTERPRETATION

The results of data analysis in this chapter are divided into 6 sections; Top depth structure map and net sand map, Allan diagram, SGR calculation, across-fault pressure difference and pore pressure profile, identification of mineral composition and fault seal calibration diagram. The analytical results and interpretations are described below.

4.1 Top depth structure map and net sand map

Top depth structure map of reservoir sand horizon are assigned as 2.5 x 4 km. for X and Y, respectively. These maps comprise the sand horizons 460, 400, 330, 250, 200 and 140 that were constructed to describe the geological structure and reservoir geometry in the study area. The Jasmine-A faults lie in a NNE-SSW trend and separated the Jasmine-A area with a high throw, steeply dipping fault (80-85°), into three main areas; the upthrown area which is the central fault block area and the downthrown areas which are the west and the east blocks. The thickness of sand reservoirs in the Jasmine A area are in range of 39 to 102 ft in the upthrown side, 23 to 92 ft in the western downthrown side and 38 to 83 ft in the eastern downthrown side.The high sand thickness (> 50 ft) appears at the sand horizon 200 (Figure 4-5b) which is a sheet of sand covering the western downthrown area. The top depth structure map and the net sand map of six reservoir sand horizons are shown in Figures 4-2 to Figure 4-7.

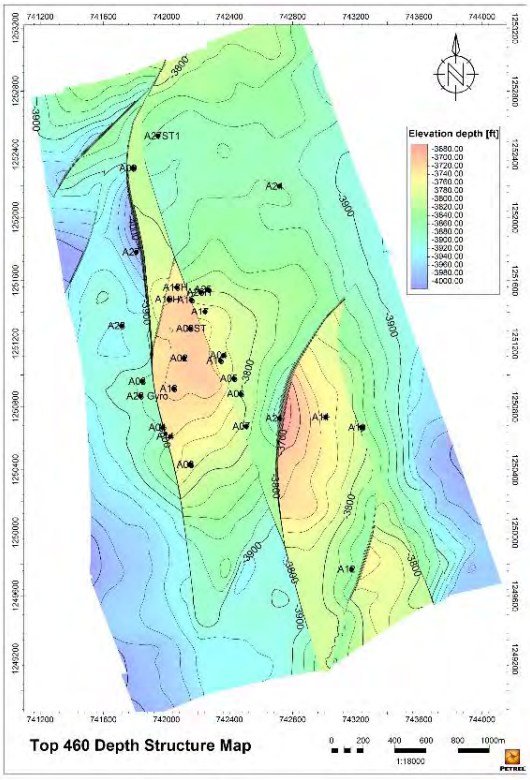

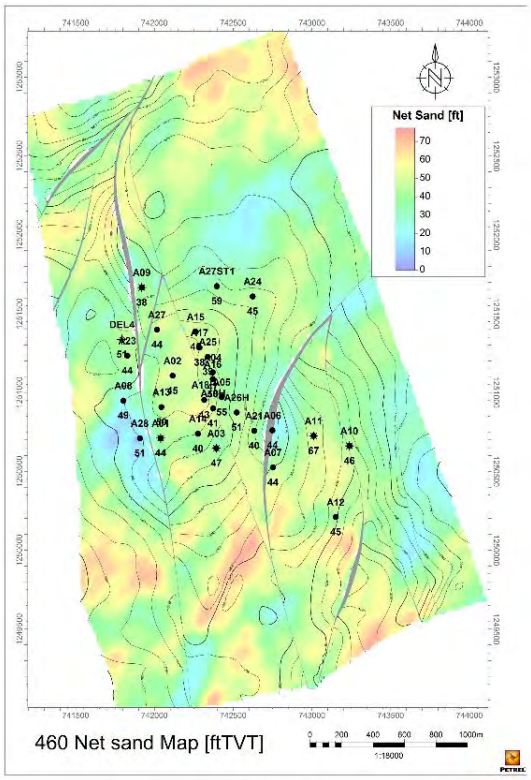

Figure 4-1 (a) Top 460 depth structure map of Jasmine A area.

(b) 460 net sand map of Jasmine A area.

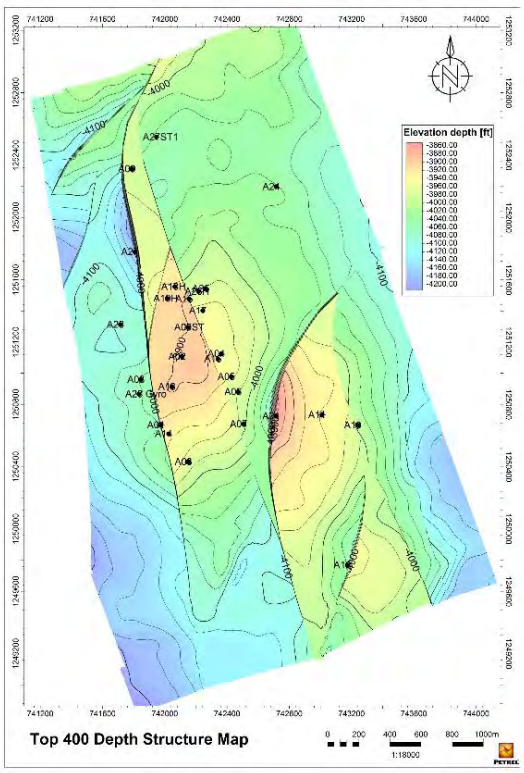

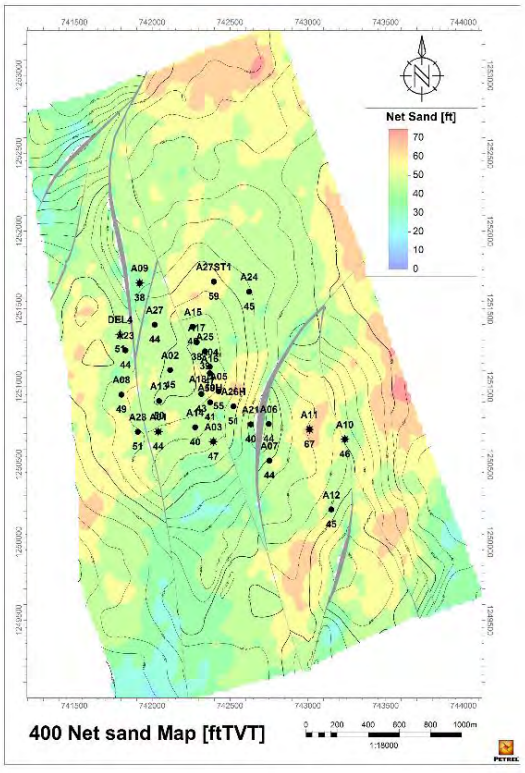

Figure 4-2 (a) Top 400 depth structure map of Jasmine A area.

(b) 400 net sand map of Jasmine A area.

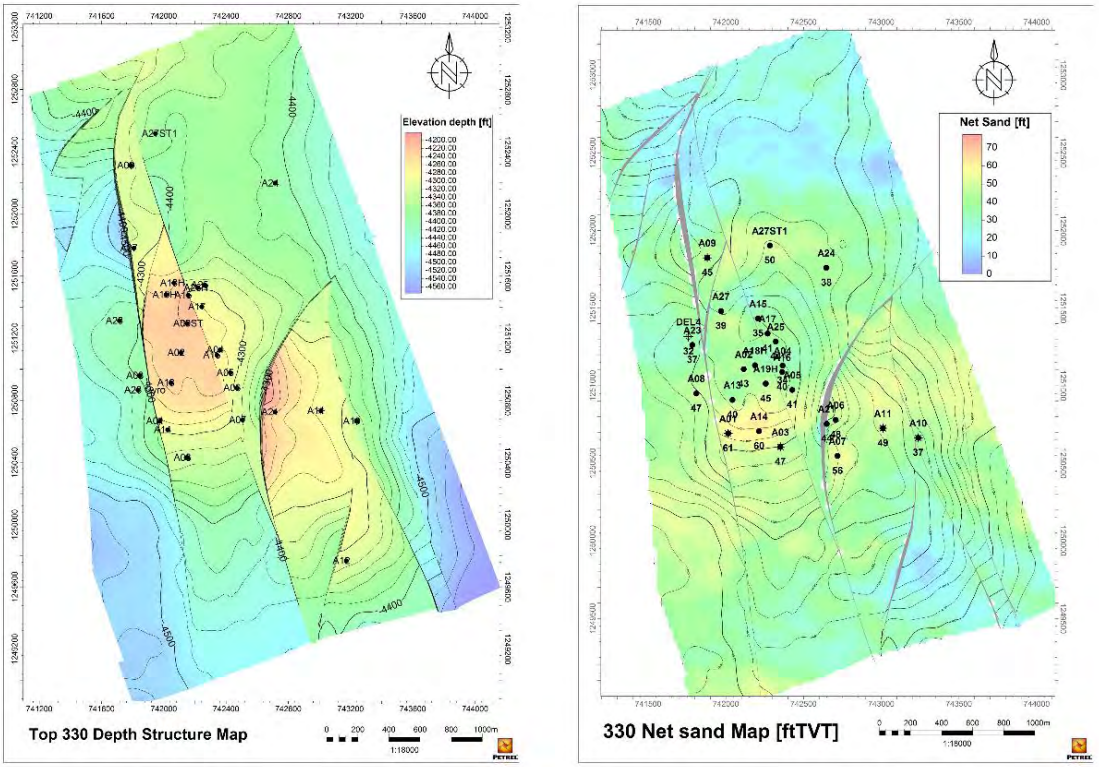

Figure 4-3 (a) Top 330 depth structure map of Jasmine A area.

(b) 330 net sand map of Jasmine A area.

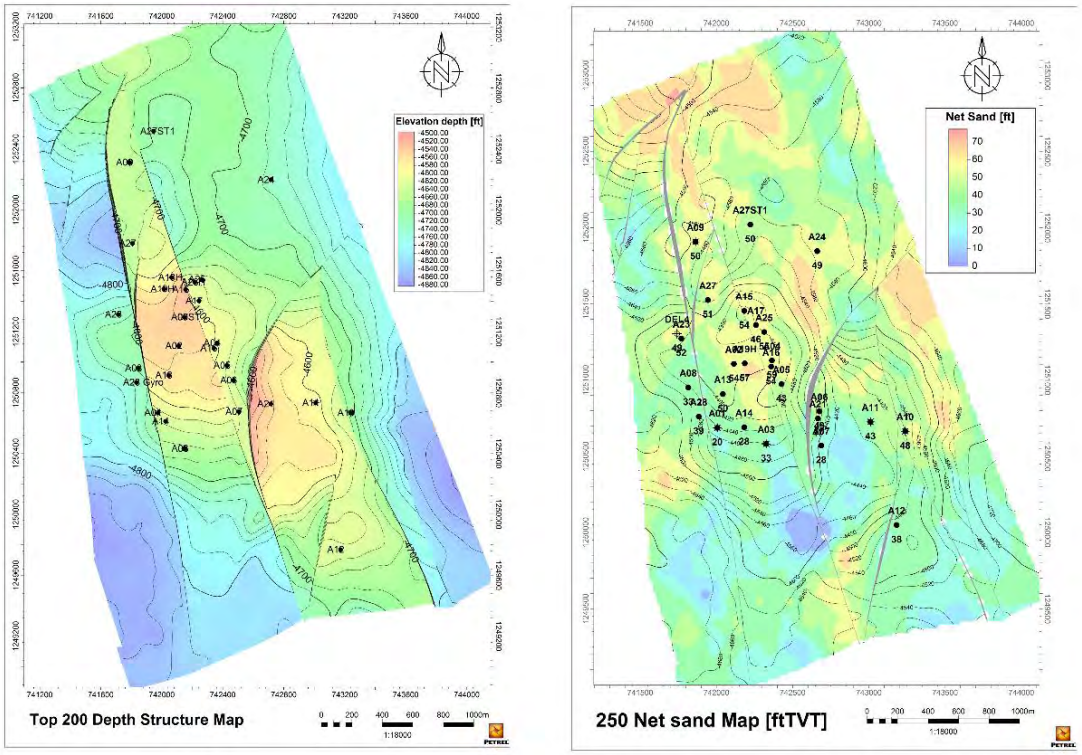

Figure 4-4 (a) Top 250 depth structure map of Jasmine A area.

(b) 250 net sand map of Jasmine A area.

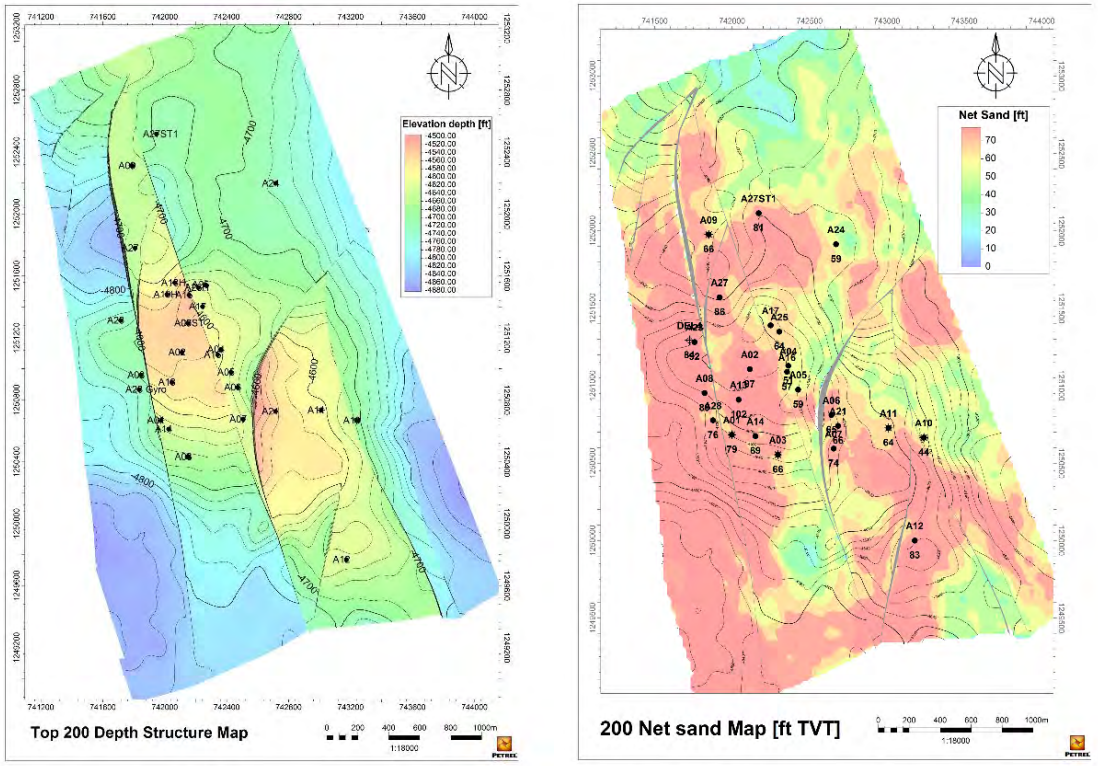

Figure 4-5 (a) Top 200 depth structure map of Jasmine A area.

(b) 200 net sand map of Jasmine A area.

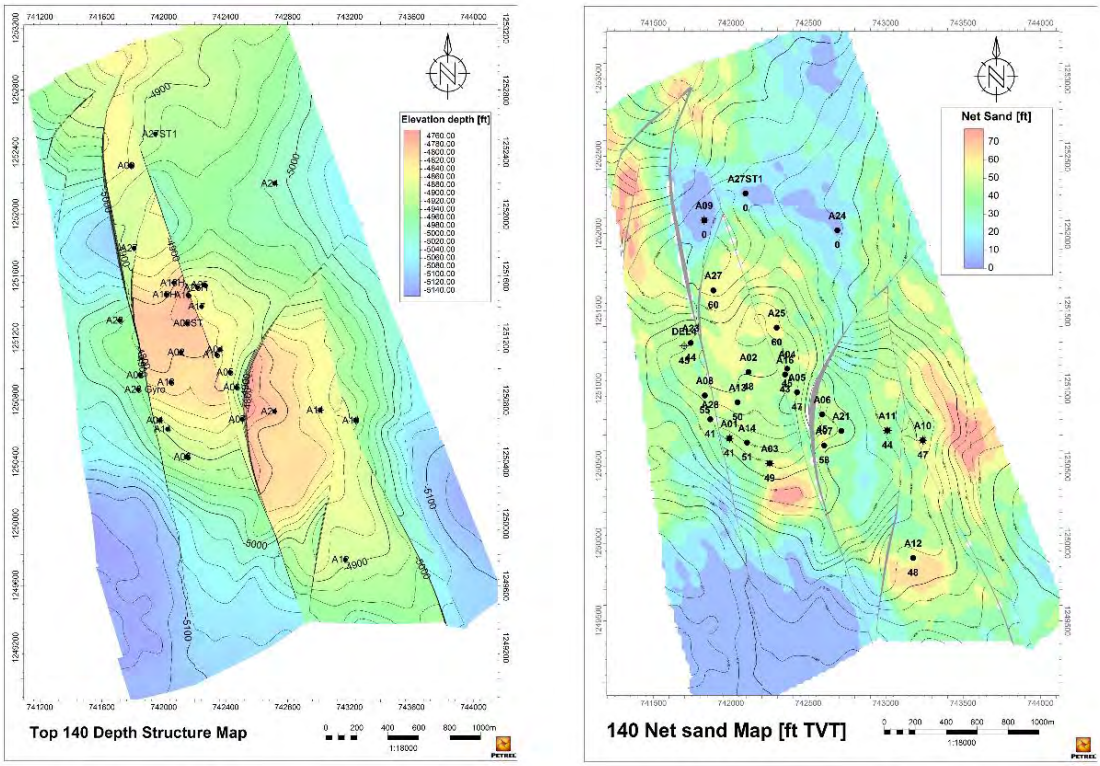

Figure 4-6 (a) Top 140 depth structure map of Jasmine A area.

(b) 140 net sand map of Jasmine A area.

4.2 Allan diagram

Allan diagram illustrated the analytical section of fault plane for trapping and lateral sealing. In this study, Allan diagrams were constructed from the top depth structure and the net sand maps for faults JA-1 and JA-2 as shown in Figure 4-7 and Figure 4-8. The maximum fault throw of fault JA-1 and JA-2 are 180 and 90 ft, respectively. The distance along the strike of faults, both fault JA-1 and fault JA-2 are 2700 ft which is used to analyse the potential of hydrocarbon sealing on the faults in the study area. The potential sealing area and the leakage across-fault area can be identified into two groups; (1) sand-to-shale (reservoir to non-reservoir) juxtaposition area and (2) sand-to-sand (reservoir to reservoir) juxtaposition area which are explained as follow.

(1) Sand-to-shale (reservoir to seal) juxtaposition

Basically, the sand-to-shale juxtaposition can be recognized as the lithological sealing because the fault cannot act as an open conduit in an area where the rock layers are permeable against non-permeable. Therefore, the hydrocarbon accumulation is trapped without any leakage zone.

(2) Sand-to-sand (reservoir to reservoir) juxtaposition

The sand-to-sand juxtaposition is generally considered as a leakage fault which is a suitable migration pathway along bedding plane to upward position while lack of closures. However, the hydrocarbon can be trapped in situation where clay smears have generated along the fault plane and trap hydrocarbon along the fault. This case have to investigate the potential of hydrocarbon sealing to check the community of fluids between sand-to-sand juxtaposition.

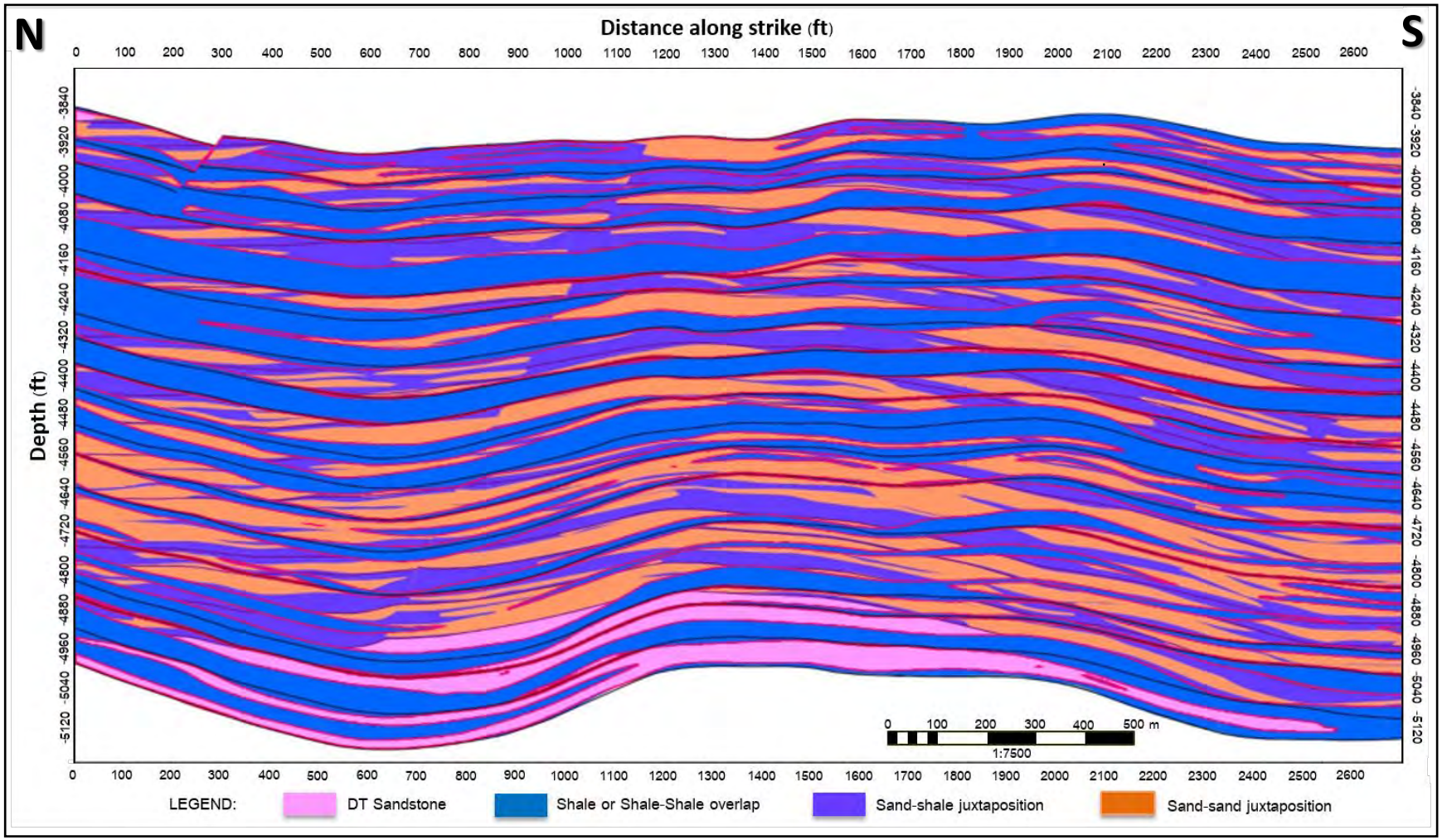

Figure 4-7 Allan diagram of fault JA-1 illustrates the reservoir sand horizons juxtaposed against the other sand horizons across a fault which is represented by the purple color and the sand horizons juxtaposed against clay/shale bed across a fault represented by the orange color.

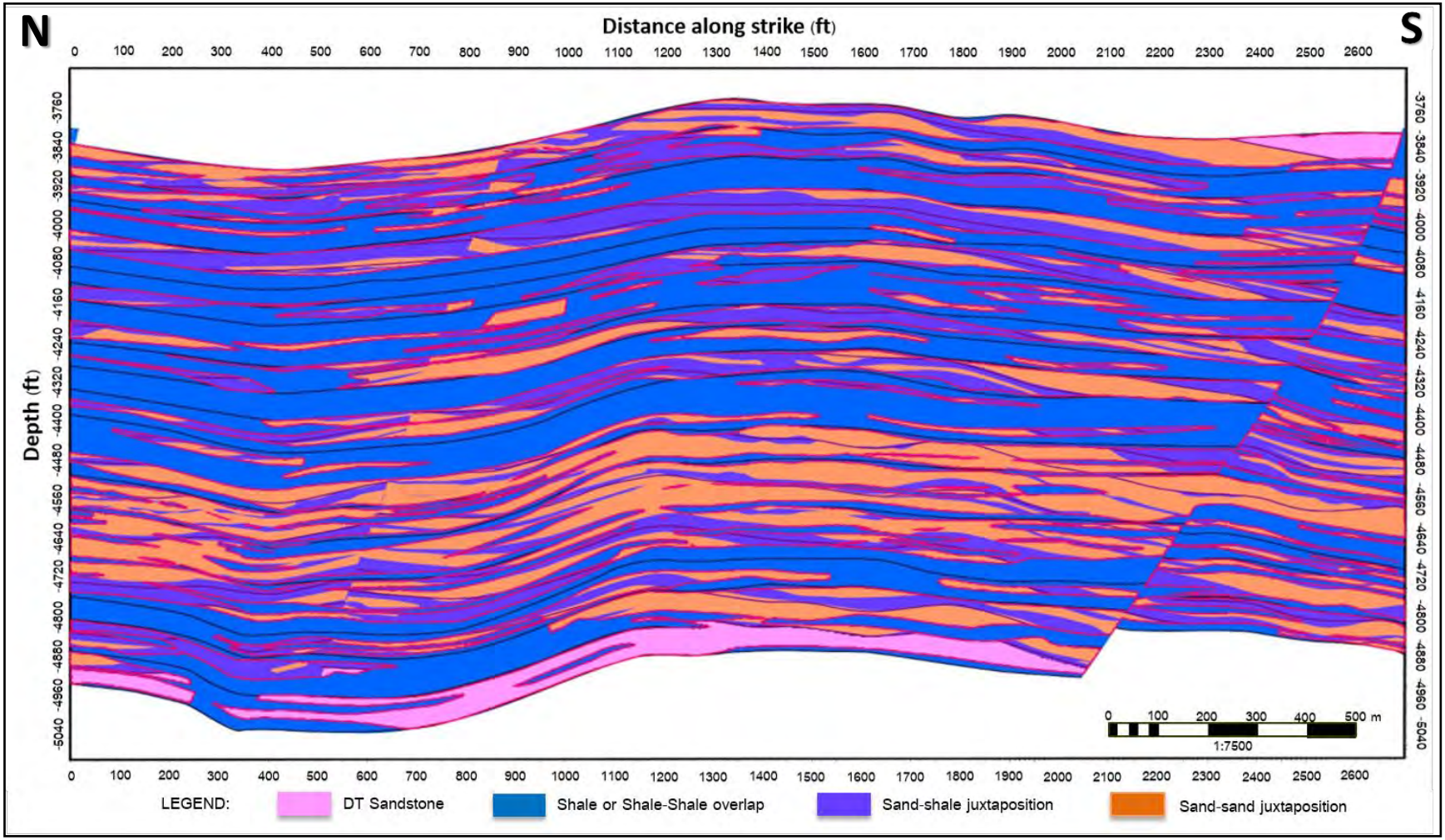

Figure 4-8 Allan diagram of fault JA-2 illustrates the reservoir sand horizons juxtaposed against the other sand horizons across a fault which is represented by the purple color and the sand horizons juxtaposed against clay/shale bed across a fault represented by the orange color.

4.3 Shale Gouge Ratio (SGR)

The SGR value calculated from the triangle diagram will be considered only in the case of sand horizons juxtaposed against the other sand across a fault because the area of sand on sand juxtaposition can be considered as a fault leakage unit. For the sand horizon juxtaposed against clay/shale bed across a fault, it is considered as a fault sealing.

The SGR value in this research is calculated from the average SGR value of the wells JA-23 and JA-27, and the wells JA-16 and JA-27, for the fault JA-1 and fault JA-2, respectively. The results of SGR value of both faults calculated from the triangular diagram are shown in Figures 4-9, 4-10, 4-11 and the average SGR value displayed on the Allan diagram (Figure 4-12 and Figure 4-13) are ranging from 22-52% for the fault JA-1 and 19-66% for the fault JA-2. The various proportion of the SGR in the triangle diagram in this research refers to the interval of SGR value from the manual of Badleys's Triangle software displayed in the same interval. SGR color-coding for SGR (modified from Triangle software manual, 2001) is shown below.

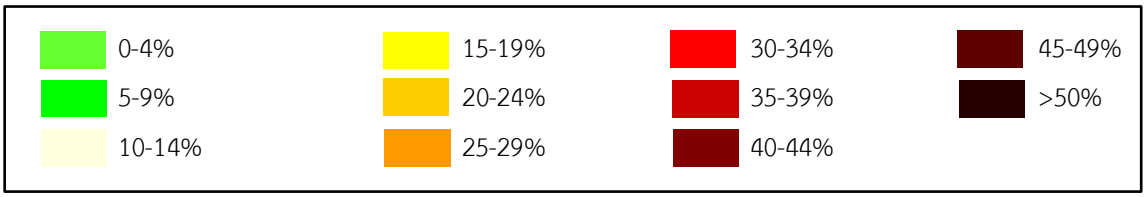

The SGR value which is cut off at 20% in the triangle diagram will indicate the leakage area in the fault zone. Therefore, all the sand-to-sand juxtaposition area of the faults in Jasmine A are potential hydrocarbon sealing areas. Moreover, this area can be indicated as a potential area due to the minimum of SGR value in Jasmine A-fault is higher than 20% which can represent fault seal by clay smears mechanism. Thus, the faults in Jasmine A area have a high probability to generate clay smear along the fault plane and trap hydrocarbon along the faults. However, there is the uncertainty of SGR calculation because of the clay volume, fault throw, and fault rock characteristics.

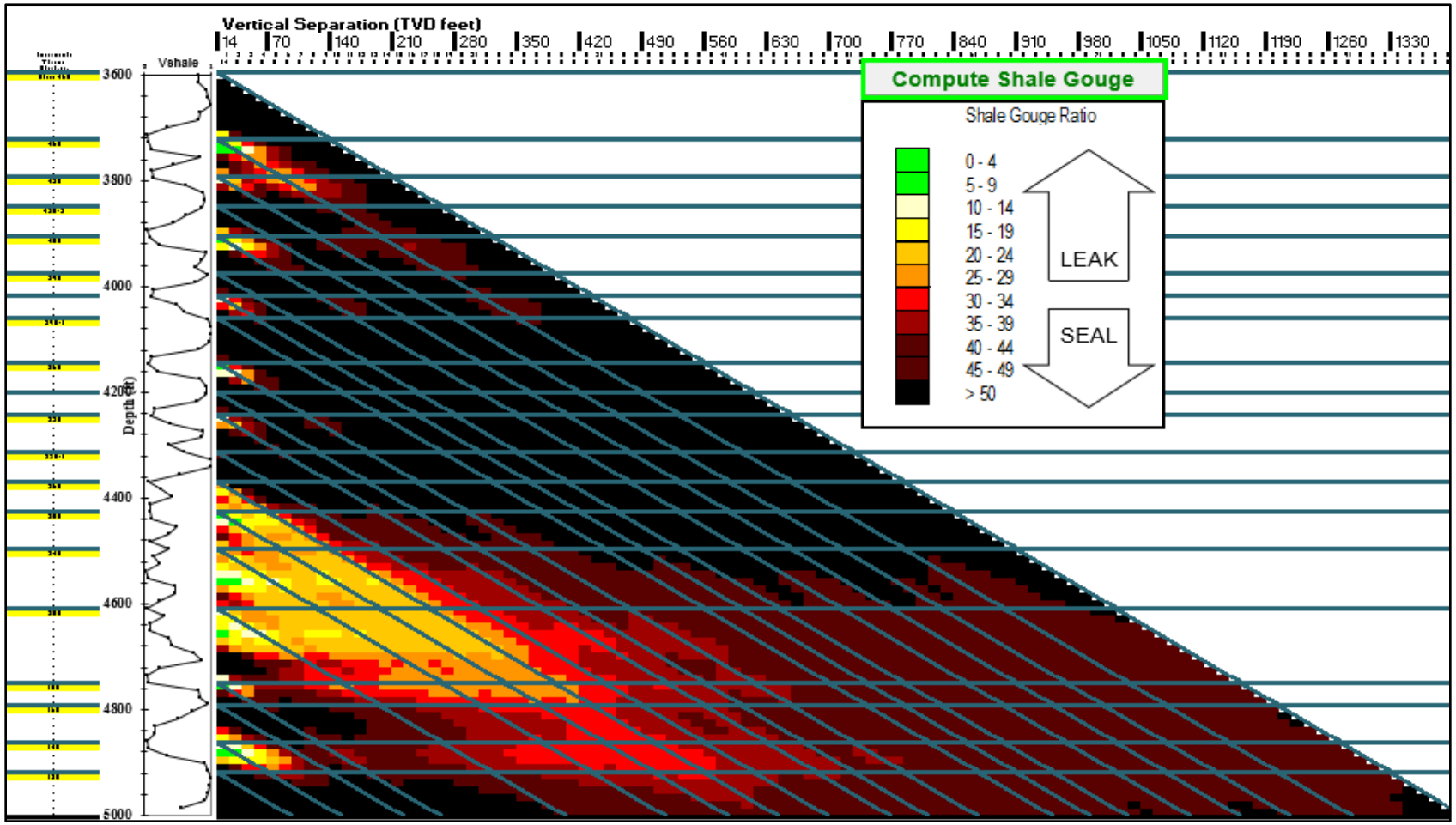

Figure 4-9 Triangle diagram of well JA-27, which is the upthrown side of both fault JA-1 and fault JA-2, illustrates the various proportion of the shale gouge ratio (SGR) value with the fault throw and sand horizon depth. The SGR value is calculated by using the volume of clay (Vcl.) from well JA-27. The horizontal lines represent the upthrown side of the reservoir zone and the diagonal lines represent the downthrown side of the reservoir zone.

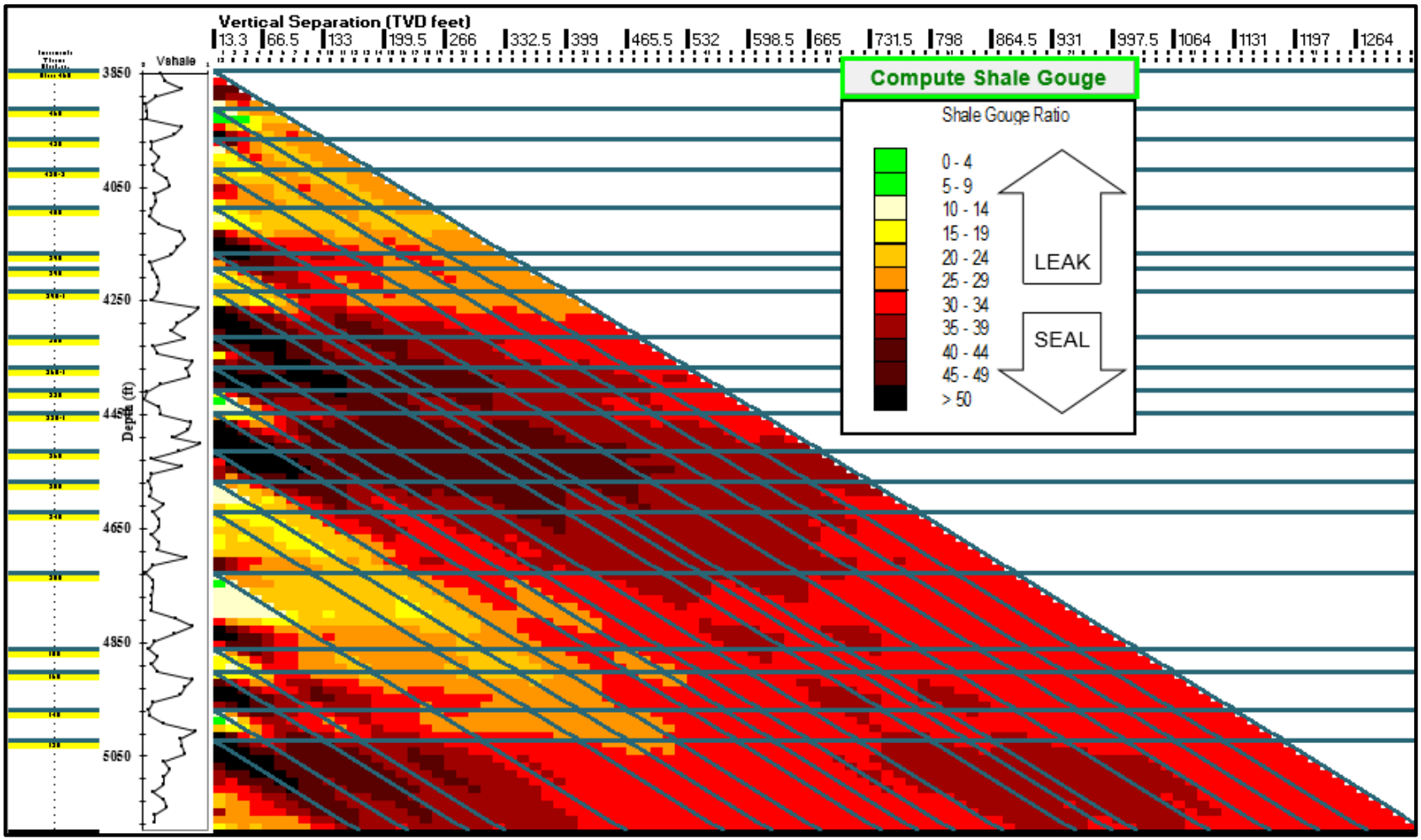

Figure 4-10 Triangle diagram of well JA-23, which is the downthrown side of fault JA-1, illustrates the various proportion of the SGR value with the fault throw and sand horizon depth. The SGR value is calculated by using the volume of clay (Vcl.) from well JA-23. The horizontal lines represent the upthrown side of the reservoir zone and the diagonal lines represent the downthrown side of the reservoir zone.

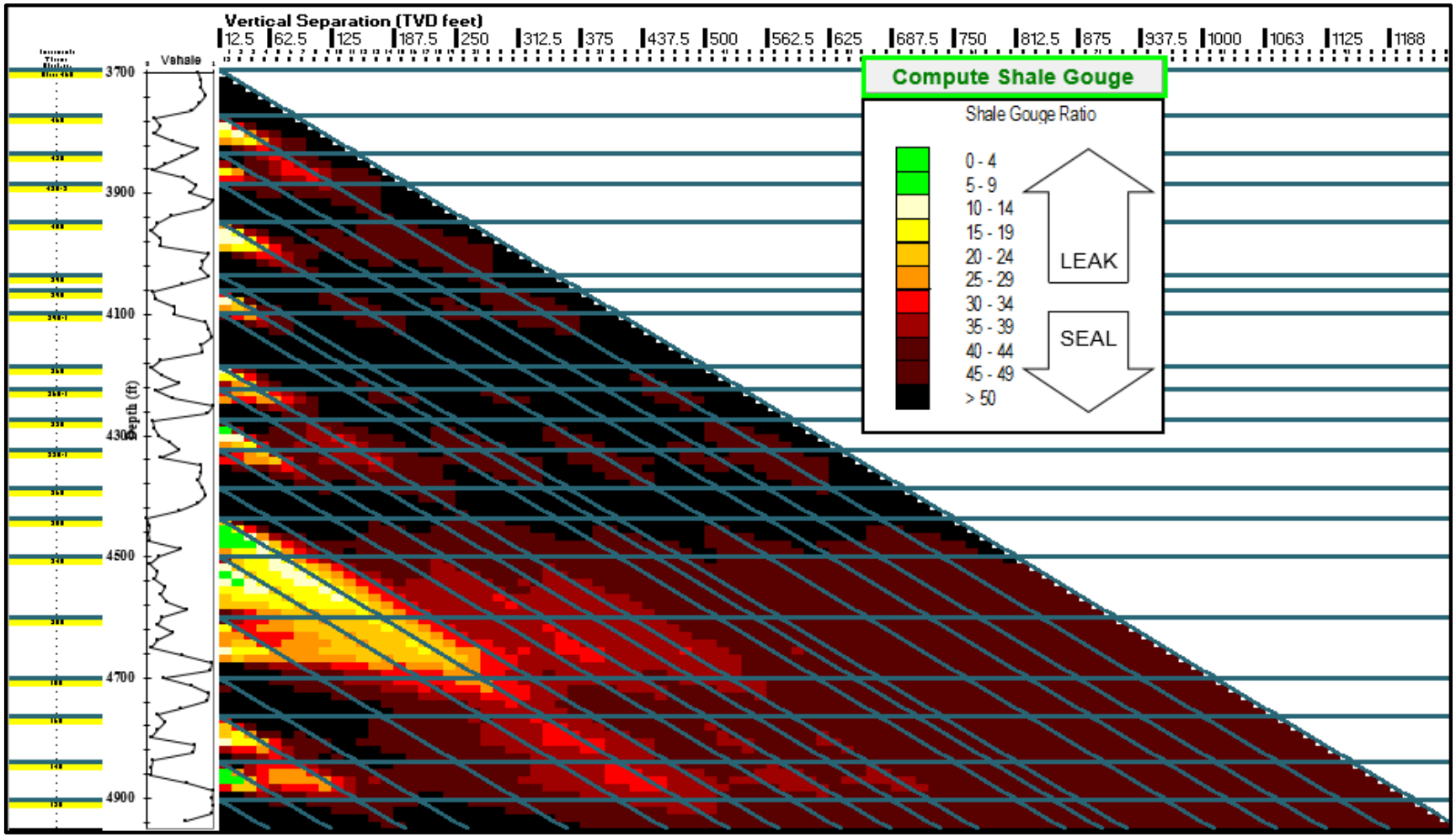

Figure 4-11 Triangle diagram of well JA-16, which is the downthrown side of fault JA-2, illustrates the various proportion of the SGR value with the fault throw and sand horizon depth. The SGR value is calculated by using the volume of clay (Vcl.) from well JA-16. The horizontal lines represent the upthrown side of the reservoir zone and the diagonal lines represent the downthrown side of the reservoir zone.

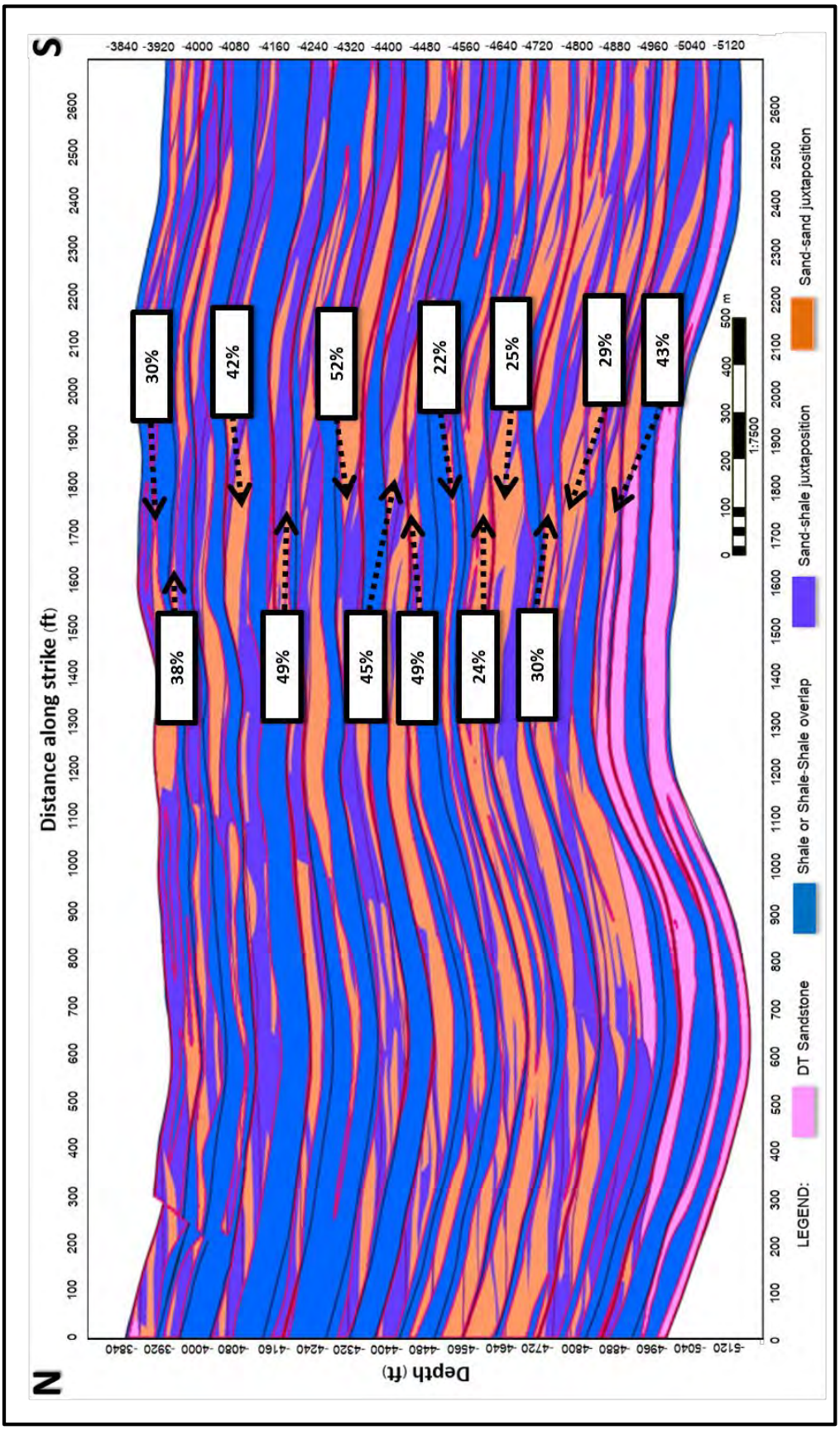

Figure 4-12 Allan diagram showing the SGR value of the sand-to-sand juxtaposition area for the fault JA-1.

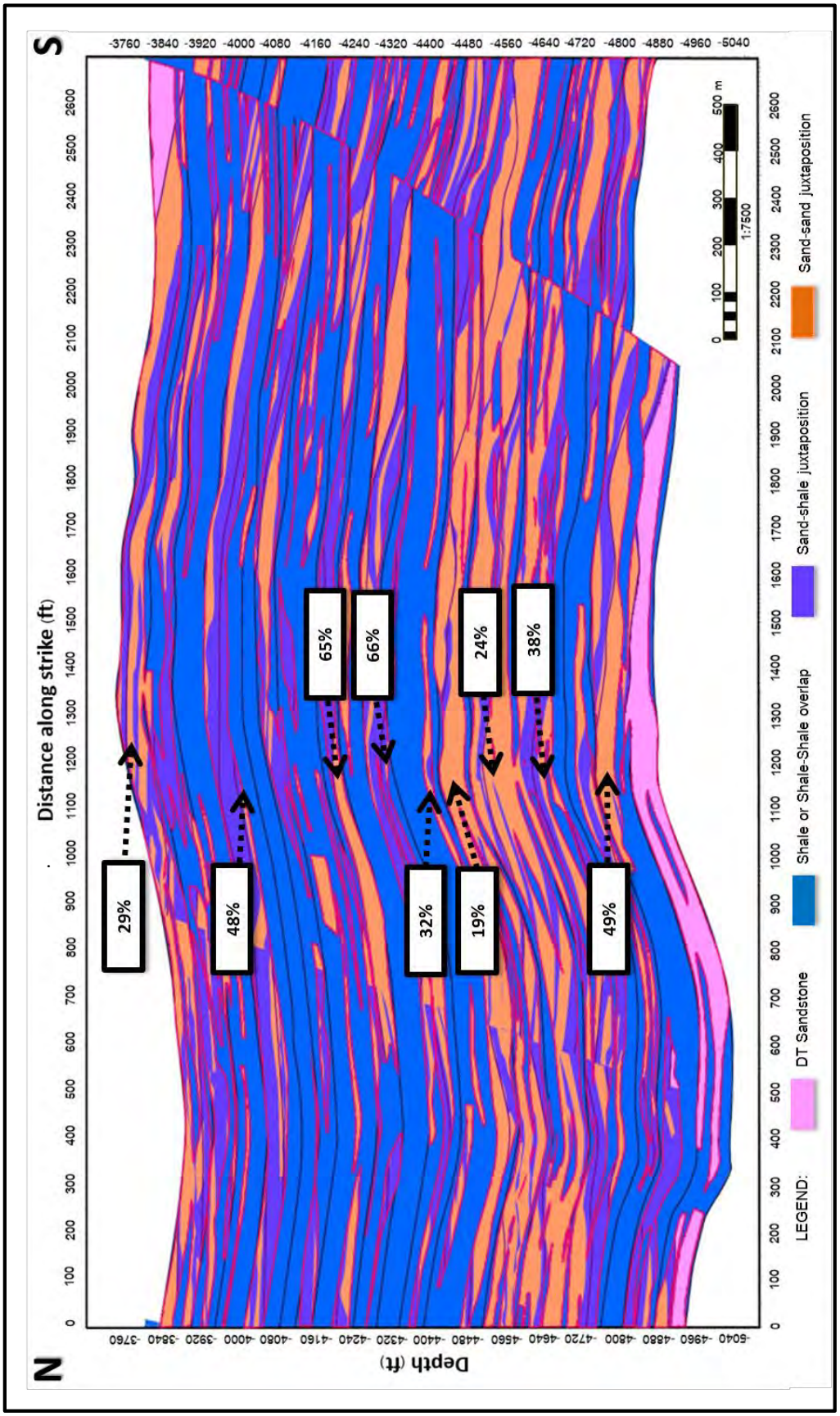

Figure 4-13 Allan diagram showing the SGR value of the sand-to-sand juxtaposition area for the fault JA-2.

4.4 Across-fault pressure difference and pore pressure profile.

The results of across-fault pressure difference and the pore pressure profile in this study are divided into two sections; Across-fault pressure difference and pore pressure profile of the 6 sand horizons. The details of analysis and the pressure distribution in each horizon in the Jasmine A area are described as follows.

4.4.1 Across-fault pressure difference

The across-fault pressure difference (ΔP) which measure and calculate from the pore-pressure profile using the pressure data of 4 wells; well JA-02, JA-03, JA-05 and DL-4 which are the pre-production wells are shown in Table 4-1 as below.

Table 4-1 Across-fault pressure difference of fault JA-1 and fault JA-2.

Fault JA-1			**Fault JA-2**		
Pressure of sand reservoir horizon (psi)		**Pressure difference, ΔP (psi)**	**Pressure of sand reservoir horizon (psi)**		**Pressure difference, ΔP (psi)**
Upthrown	**Downthrown**		**Upthrown**	**Downthrown**	
1694.16	1689.41	4.75	1628.14	1632	3.86
1805.66	1814.59	8.93	1814.18	1809.25	4.93
1848.54	1868.27	19.73	1852.75	1857.8	5.05
1909.08	1907.66	1.42	1908.25	1910.66	2.41
1938.59	1956.43	17.84	1938.2	1939.04	0.84
1963.57	1971.68	8.11	1988.58	1991.13	2.55
2046.41	2044.27	2.14			

4.4.2 Pore pressure profile

The pore pressure profiles analysed from RFT data in each well is used to construct the pore pressure profile in the Jasmine A area (Figure 4-19). The RFT data of the pre-production wells JA-02 and JA-03 represent the pore pressure data in the upthrown side, well JA-05 and well DL-4 represent the pore pressure data in the western and the eastern downthrown side. The details of fluid properties in each well such as fluid gradient, fluid type and fluid contact depth are shown in Figures 4-20 to Figure 4-23.

Well JA-02

Fluid type: Gas, Oil and water

Gradient:

Gas gradient = (1) 0.104 psi/ft, Fluid contact depth: (1) GWC = -3807 ft

(2) 0.097 psi/ft, (2) GWC = -3923 ft

(3) 0.148 psi/ft, (3) GWC = -4297 ft

(4) 0.097 psi/ft, (4) GWC = -4474 ft

(5) 0.148 psi/ft, (5) GWC = -4772 ft

(6) 0.097 psi/ft, (6) GWC = -4848 ft

(7) 0.148 psi/ft, (7) GWC = -5113 ft

Oil gradient = 0.234 psi/ft, Fluid contact depth: OWC = -4225 ft

Water gradient = 0.420 psi/ft

Well JA-03

Fluid type: Oil and water

Gradient:

Oil gradient = 0.385 psi/ft, Fluid contact depth: OWC = -5198 ft

Water gradient = 0.424 psi/ft

Well JA-05

Fluid type: Gas, Oil and water

Gradient:

Gas gradient = 0.139 psi/ft, Fluid contact depth: GWC = -5117 ft

Oil gradient = 0.342 psi/ft, OWC = -4280 ft

Water gradient = 0.415 psi/ft

Well DL-4

Fluid type: Gas, Oil and water

Gradient:

Gas gradient = (1) 0.104 psi/ft, Fluid contact depth: (1) OWC = -4358 ft

(2) 0.097 psi/ft, (2) OWC = -4439 ft

(3) 0.148 psi/ft, (3) OWC = -4763 ft

Oil gradient = 0.315 psi/ft, Fluid contact depth: OWC = -4229 ft

Water gradient = 0.415 psi/ft

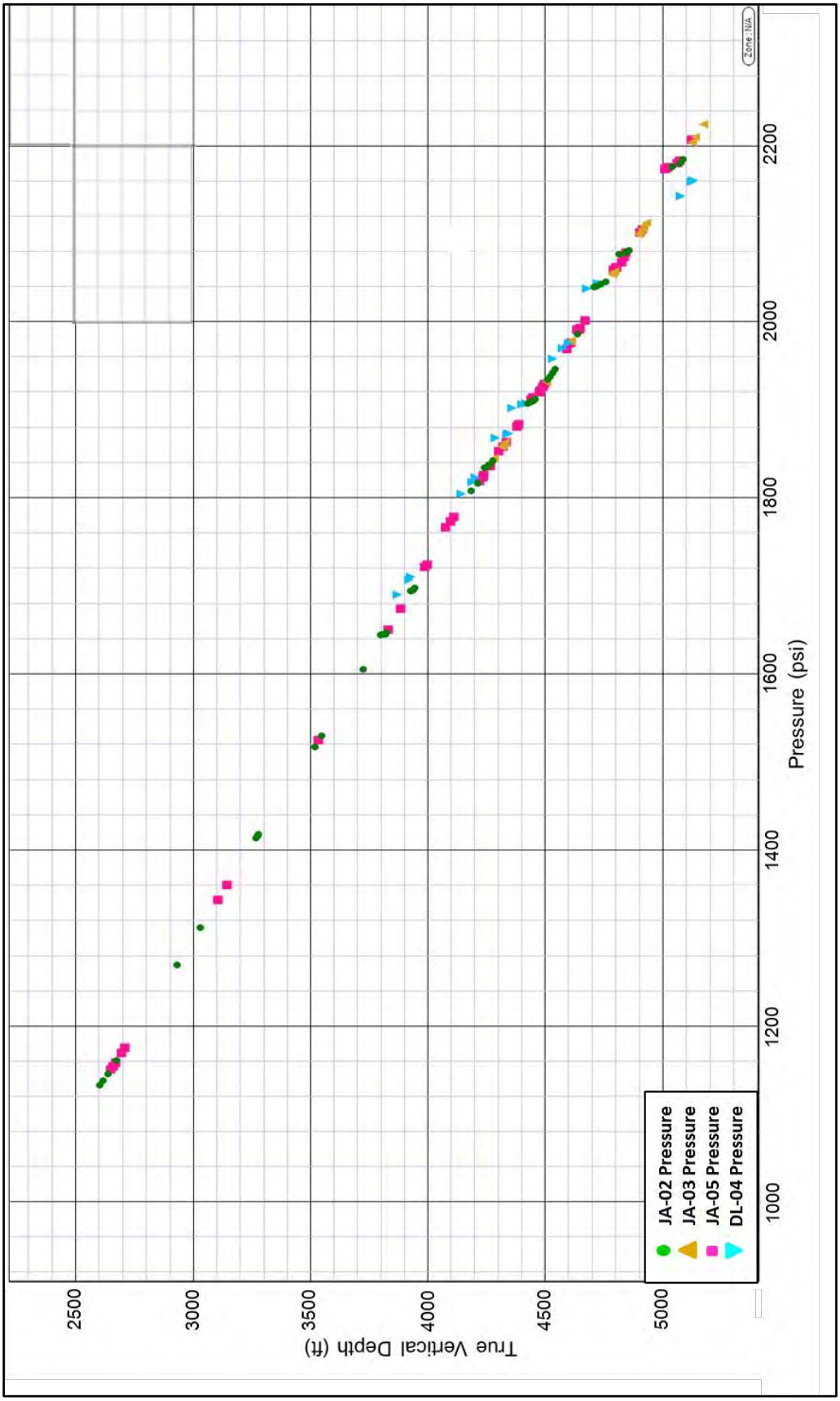

Figure 4-14 Pore pressure profile using RFT data of 4 wells; well JA-02, JA-03, JA-05 and DL-4 shown pore pressure distribution in Jasmine A area.

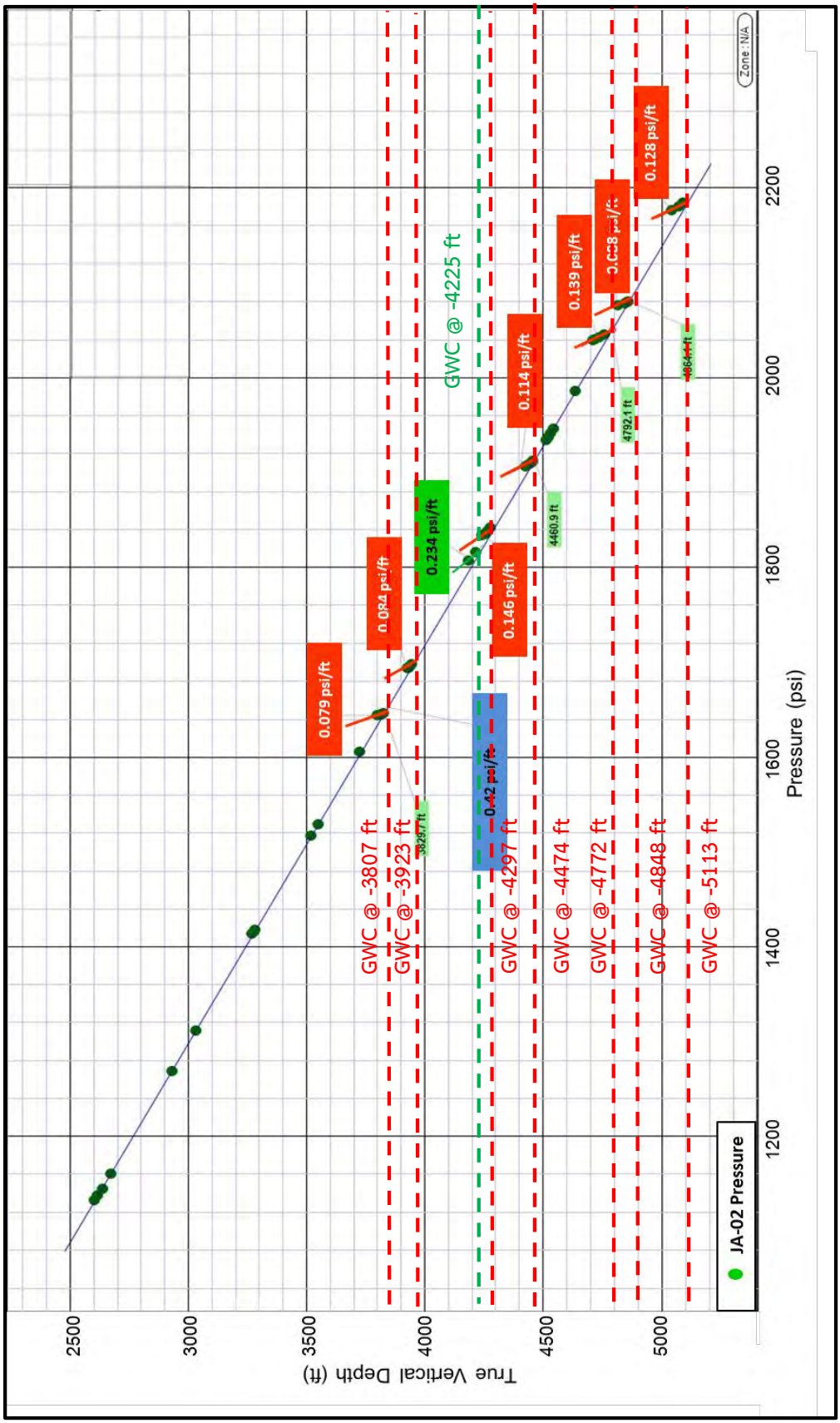

Figure 4-15 Pore pressure profile showing pore pressure distribution of the well JA-02 which represents the pore-pressure in the upthrown side.

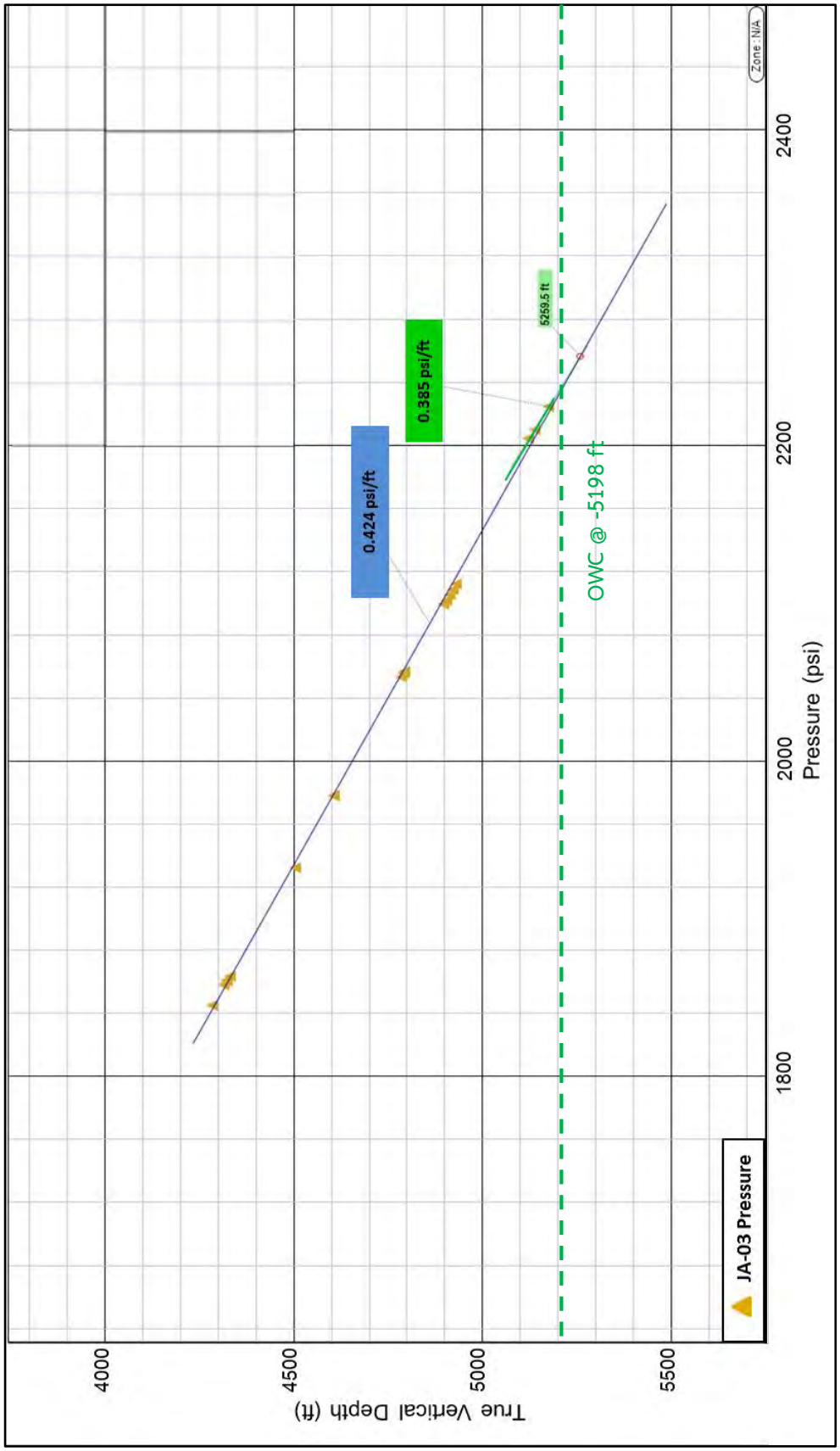

Figure 4-16 Pore pressure profile showing pore pressure distribution of the well JA-03 which represents the pore pressure in the upthrown side.

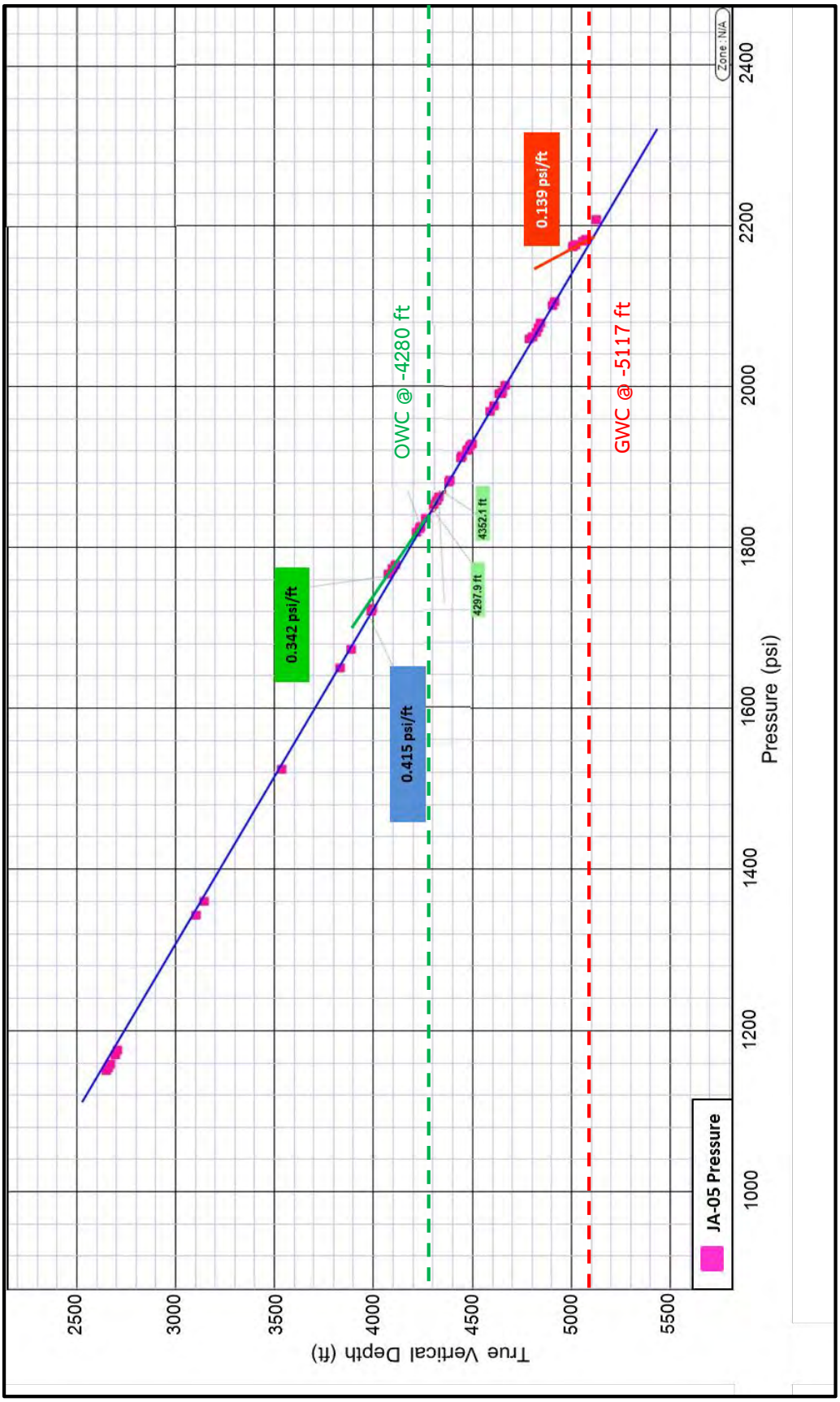

Figure 4-17 Pore pressure profile showing pore pressure distribution of the well JA-05 which represents the pore pressure in the eastern downthrown side.

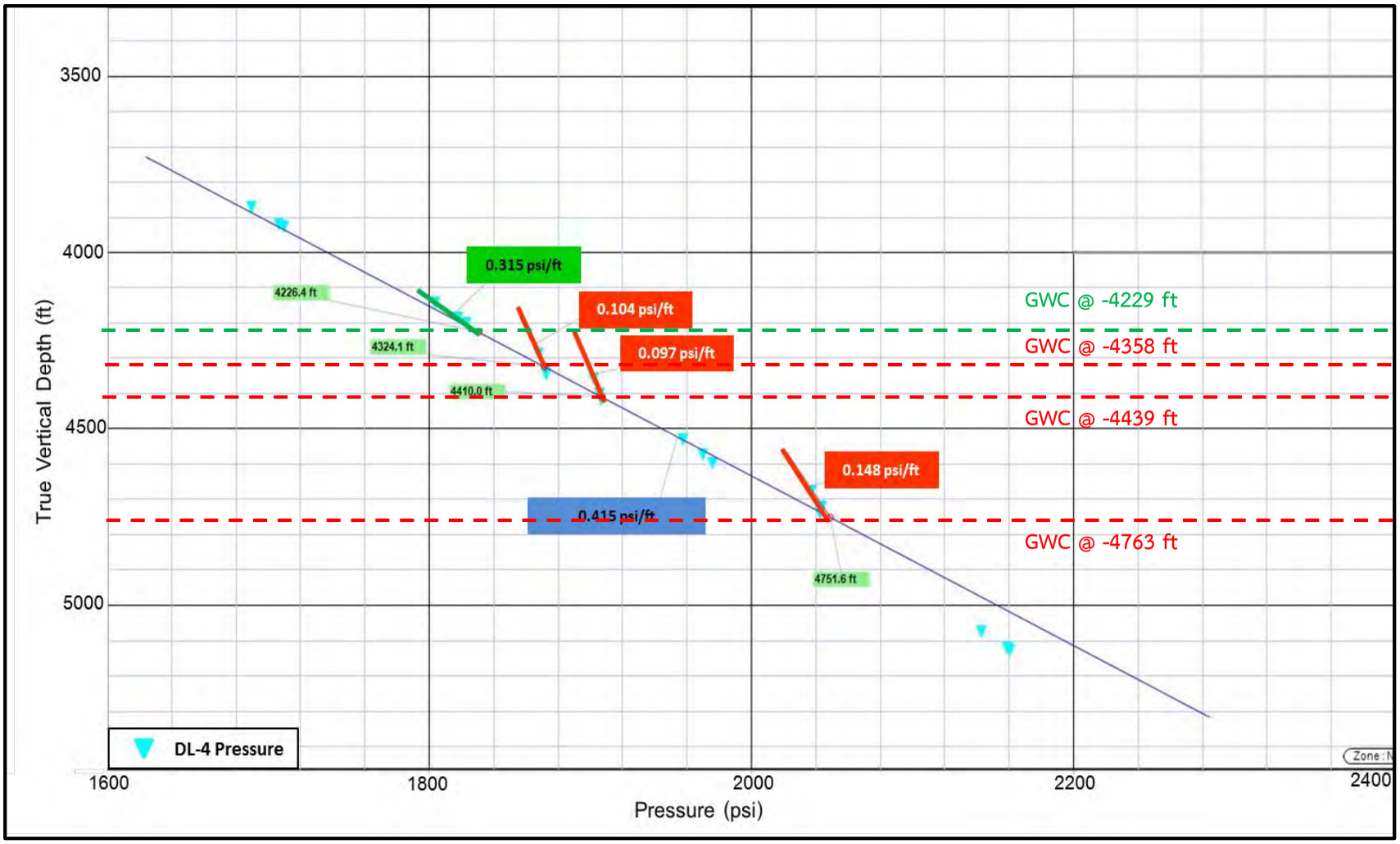

Figure 4-18 Pore pressure profile showing pore pressure distribution of the well DL-4 which represents the pore pressure in the western downthrown side.

4.5 Mineral composition

The samples are composed of quartz 82.36% and other minerals 17.63% (Table 4-2). The grain particles vary from angular to round and have low to medium sphericity. For the results of XRD analysis, there are three major minerals which comprise quartz (71.033 wt%), calcite (12.162 wt%), and dolomite (16.805 wt%). Physical property and XRD analysis of the samples are shown in Table 4-2, Figure 4-24, 4-25, Table 4-3 and Figure 4-26, respectively.

Table 4-2 Physical property and mineral composition of the samples from well JA-23 and well JA-27.

Samples	Depth interval (ft)	% Mineral		Sphericity	Roundness
		Quartz	Other minerals		
JA-23-1	5500-5560	75	25	Low	Angular to sub-rounded
JA-23-2	5620-5680	82	18	Medium	Angular to sub-rounded
JA-23-3	5860-5920	80	20	Low	Sub-angular to sub-rounded
JA-23-4	6040-6100	88	12	Low	Angular to sub-rounded
JA-23-5	6220-6280	87	13	Medium	Sub-angular
JA-27-1	5020-5050	80	20	Medium	Sub-rounded
JA-27-2	5230-5260	89	11	Medium	Sub-angular to sub-rounded
JA-27-3	5380-5410	79	21	Medium	Angular to sub-rounded
JA-27-4	5530-5560	73	27	Medium	Angular to sub-rounded
JA-27-5	5710-5740	86	14	Medium	Angular to sub-rounded
JA-27-6	6040-6070	87	13	Medium	Angular to sub-rounded

Figure 4-19 Photo of cutting samples from the well JA-23 (4X magnification).

Figure 4-20 Photo of cutting samples from the well JA-27 (4X magnification).

Table 4-3 Mineral composition of the samples from well JA-23 and well JA-27.

Samples	Depth interval (ft)	% Mineral		
		Quartz	Calcite	Dolomite
JA-23-1	5500-5560	70.62	18.03	11.29
JA-23-2	5620-5680	65.79	23.86	10.35
JA-23-3	5860-5920	70.15	10.83	19.02
JA-23-4	6040-6100	76.71	4.57	18.72
JA-23-5	6220-6280	77.00	4.47	18.53
JA-27-1	5020-5050	59.88	28.69	17.43
JA-27-2	5230-5260	74.79	13.16	12.05
JA-27-3	5380-5410	68.79	15.76	15.45
JA-27-4	5530-5560	49.41	8.64	41.94
JA-27-5	5710-5740	83.66	5.28	11.06
JA-27-6	6040-6070	85.56	5.42	9.02

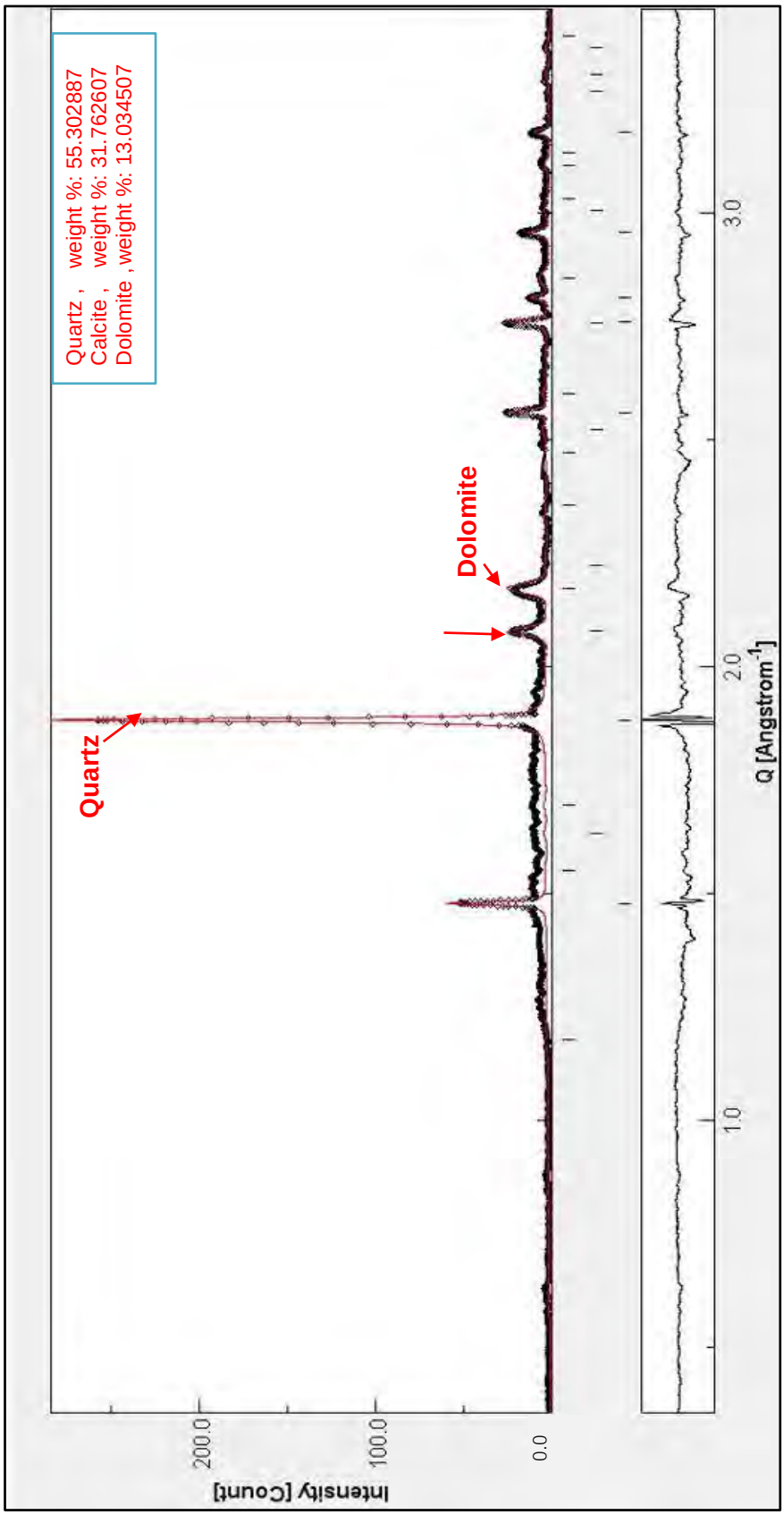

Figure 4-21 Example of XRD analysis showing the peak position of minerals.

4.6 Fault seal calibration diagram

The seal capacity on the faults in Jasmine A area is estimated by a comparison of across-fault pressure difference and the shale gouge ratio in the sand-sand overlap area. The dash line in the fault seal calibration diagram represents seal capacity of the fault and the data point which is close to the seal capacity line represents the maximum capillary entry pressure that can be supported at a specific SGR value.

The interpretation of the calibration diagram is that the area below the seal capacity line represents the fault sealing, whereas the area above the seal capacity line represents the seal failure of fault rocks (Figure 4-22). The minimum SGR of 22% can be supported by the across-fault pressure difference at 8.11 psi.

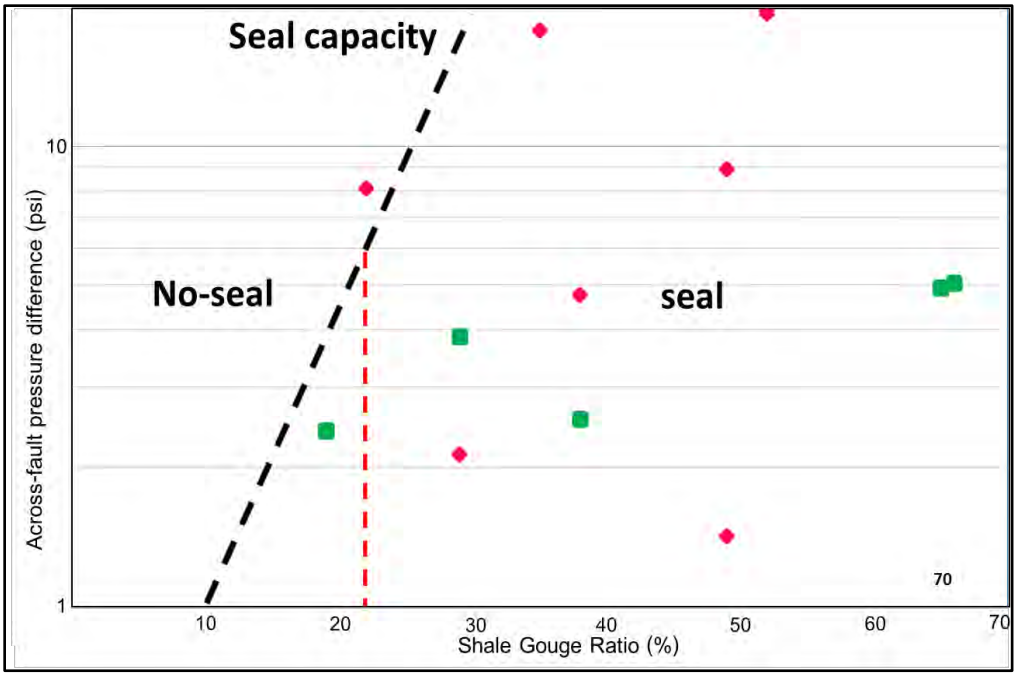

Figure 4-22 Fault seal calibration diagram for the Jasmine A area showing the relationship between across-fault pressure difference and SGR. Dash line in red color represents “seal capacity” which was derived from Yielding et al. (2002).

CHAPTER 5

DISCUSSION AND CONCLUSION

The results of the fault seal study in the Jasmine A area from the previous chapter are discussed and concluded in this chapter.

5.1 Discussion

Based on the results, there are some uncertainties of fault thrown SGR calculation due to a limitation of data for the fault seal analysis in the study area. This uncertainties are described as follows.

5.1.1 Fault throw

The limitation of fault thrown measuring is the uncertainty of mapping due to the velocity model which will be generated from the time map to the depth map.

5.1.2 SGR calculation

The threshold of the SGR value for fault sealing published by Yielding et al. (1997) is approximately 20%, whereas In this research, the SGR value cut off is 22% and can identify the fault seal capacity in the sand-to-sand juxtaposition area. However, this calculation has some uncertainty in the fault seal estimation because of the data limitation and the bin size determination in the triangle diagram.

5.1.3 Comparison of SGR calibration with the other areas

The result of the fault seal capacity of this research which is compared with SGR data provided by Yielding (2002) and Bretan et al. (2003). These data are derived from a variety of basin worldwide such as North Sea, mid-Norway, Grand Banks, Gulf of Mexico, Columbus Basin, Niger Delta, Vietnam and Gulf of Thailand. The data set for

Jasmine A area is represented by the symbol of black diamond, while rectangle symbols in the calibration plot are from basin worldwide (Figure 5-1).

As seen in the calibration plot of SGR against across-fault pressure differences, the SGR values and across-fault pressure differences of the fault in Jasmine A area occur below the seal-failure envelope (seal capacity line). Therefore, the SGR values in the Jasmine A area are consistent with the SGR variety data from the other areas. The comparison of result data with the variety data from the other areas are shown as a diagram below.

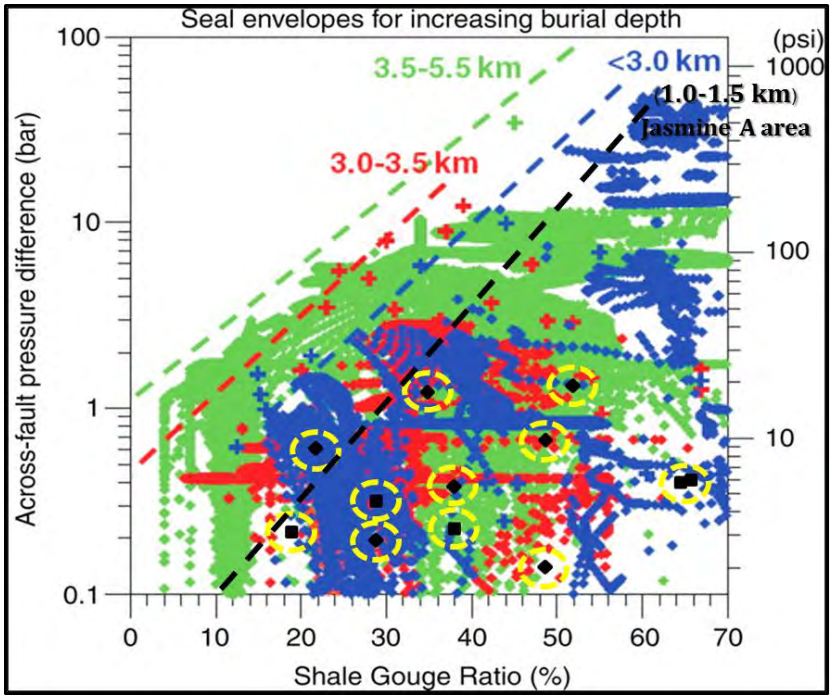

Figure 5-1 Comparison of SGR against across-fault pressure difference in the Jasmine A area with the other areas. The red, green, blue and black dash lines represent the burial depth of basins and the Jasmine A area located on the northwestern part of the Pattani Basin, Gulf of Thailand. The red, green, blue and black dots represent a variety fault data from basins worldwide and the fault data of Jasmine A area (Yielding (2002); Bretan et al. (2003)).

5.2 Conclusion

In conclusion, Allan diagram and SGR can be used to analyze and evaluate fault sealing in the Jasmine A area, which is located on the Northern part of the Pattani Basin, Gulf of Thailand.

Allan diagrams, which were constructed to show an overview of potential leak and seal points on the fault plane, can evaluate hydrocarbon accumulation efficiency along faults in Jasmine A area. As seen in the SGR calculation and the across-fault pressure difference estimation, SGR value which ranges from 22 to 66% can represent the quantitative potential hydrocarbon sealing and identify the fault seal mechanism for the sand-to-sand juxtaposition area. Therefore, SGR value at 22% is the lowest proportion which can support the across-fault pressure difference at 8.11 psi and a SGR which is lower than 22% would indicate a leakage area in the sand horizon juxtaposed against the other sand horizon across the fault plane in Jasmine A area.

Furthermore, the methodology and the result in this research can be applied to predict and evaluate the fault seal capacity in the other areas of similar lithologies and structures and also help to investigate the potential of hydrocarbon accumulation.

5.3 Recommendation

1) In order to identify possible migration routes and migration timing across faults in Jasmine Field, basin modelling needs to be reviewed.

2) XRD analysis of sidewall core sample will give more accurate results of clay minerals composition and content.

3) More data (e.g. pressure data and SGR) will better help in estimating leaking points.

REFERENCES

Allan U.S., 1989. Model for Hydrocarbon Migration and Entrapment within Faulted Structures. American Association of Petroleum Geologists Bulletin, 73(7): pp. 803-811.

Bense V.F., Van Balen, R.T. de Vries, J.J, 2003. The impact of faults on the hydrogeological conditions in the Roer Valley Rift Sytem: an overview. Netherlands Journal of Geosciences, 82(1): pp. 41 – 45.

Bretan, P., G. Yielding, and H. Jones, 2003. Using calibrated shale gouge ratio to estimate hydrocarbon column heights: AAPG Bulletin, 87: pp. 397–413.

Bustin, R.M., Chonchawalit, A., 1995. Formation and tectonic evolution of the Pattani Basin, Gulf of Thailand. International Geology Review, 37:pp. 866–892.

Cerveny K., Davies R., Dudley G., Fox R., Kaufman P., Knipe R. et al., 2004. Reducing Uncertainty with Fault-Seal Analysis. Oilfield Review, pp.38–51.

Charusiri, P., Kosuwan, S., and Imsamut, S., 1997. Tectonic evolution of Thailand: from Bunopas's model to a new scenario. In Proceedings of the International Conference on Stratigraphy and Tectonic Evolution of Southeast Asia and the South Pacific (Geothai'97), 19-24 August 1997, Bangkok, pp. 414-420.

Dahlberg, E. C. 1995. Fluids, Pressure, and Gradients. Applied Hydrodynamics in Petroleum Exploration 2: pp. 1-14.

Fisher QJ; Knipe RJ ,1998, Fault sealing processes in siliciclastic sediments, Faulting and fault sealing in hydrocarbon reservoirs, 147: pp.117-134.

Gibson, R.G., 1998. Physical character and fluid-flow properties of sandstone-derived fault gouge. In: M.P. Coward, T.S. Daltaban and H. Johnson (Editors), Structural Geology in Reservoir Characterization. Geol. Soc., Spec. Publ., 127: pp. 83–97.

Jardine, E. 1997. Dual Petroleum Systems Governing the Prolific Pattani Basin, Offshore Thailand. International Conference on Stratigraphy and Tectonic Evolution of Southeast Asia and the South Pacific, Department of Mineral Resources, Bangkok, Thailand, pp. 525-534.

Knipe, R. J., 1997. Juxtaposition and Seal Diagrams to Help Analyze Fault Seals in Hydrocarbon Reservoirs. American Association of Petroleum Geologists Bulletin, 81(2), pp.187-195.

Knipe, R.J., Fisher, Q.J., Jones, G. Clennell, M.R. Farmer, A.B., Harrison, A., White, E. A., 1997. Fault seal analysis: Successful methothologies, application and future directions. In: p. Moller-pederson, and A.G. Koesther (Eds.). Hydrocarbon Seals, NPF Special publication, 7: pp.15-38.

Koednok Thammasak, 2002. Influence of Clay and Shale Smear in Fault Zone on The Potential Sealing of Hydrocarbon in Block B8/32, Pattani Basin, Gulf of Thailand. Master's Thesis, Department of Geology, Faculty of Science, Chulalongkorn University.

Kornsawan, A., Morley, C.K., 2002. The origin and evolution of complex transfer zones (graben shifts) in conjugate fault systems around the Funan Field, Pattani basin, Gulf of Thailand. Journal of Structural Geology, 24: pp. 435–449.

Morley, C.K., Wonganan, N., 2000. Normal fault displacement characteristics, with particular reference to synthetic transfer zones, Mae Moh Mine, Northern Thailand. Basin Research, 12: pp. 1–22.

Morley, C.K., 2001. Combined escape tectonics and subduction rollback back arc extension: a model for the evolution of Tertiary rift basins in Thailand, Malaysia and Laos. Journal of the Geological Society of London, 158: pp. 461–474.

Morley, C. K. 2004. Nested strike-slip duplexes, and other evidence for Late Cretaceous-Paleogene transpressional tectonics before and during India Eurasia collision, in Thailand, Myanmar and Malaysia, Journal of the Geological Society of London, 161: pp. 799-812.

Polachan, S., Pradidtan, S., Tongtaow, C., Janmaha, S., Intarawijitr, K., Sangsuwan, C., 1991. Development of Cenozoic basins in Thailand, Marine and Petroleum Geology, 8: pp.84–97.

Vavra, C.L., J.G. Kaldi, and R.M. Sneider, 1992. Geological applications of capillary pressure: a review: AAPG Bulletin, 76: pp. 840–850.

Watts, N. L. 1987. Theoretical aspects of cap-rock and fault seals for single and two-phase hydrocarbon columns. Marine and Petroleum Geology, 4: pp. 274-307.

Watcharanantakul, R., Morley, C.K., 2000. Syn-rift and post-rift modeling of the Pattani Basin, Thailand: evidence for a ramp-flat detachment. Marine and Petroleum Geology, 17: pp. 937-958.

Williamson, C. R. 1992. Funan Field – First Gas Production From The Eastern Pattani Basin. National Conference on “Geologic Resources of Thailand: Potential for Future Development”, Department of Mineral Resources, Bangkok, Thailand, pp. 225-234.

Yielding G., 2002. Shale gouge ratio—Calibration by geohistory, in A. G. Koestler and R. Hunsdale, eds., Hydrocarbon seal quantification: Norwegian Petroleum Society Special Publication 11: pp. 1–15.

Yielding G., Freeman B. and Needham D.T., 1997. Quantitative Fault Seal Prediction. American Association of Petroleum Geologists Bulletin, 81(6): pp.897–917.

APPENDIX

XRD analysis showing the peak position of minerals.

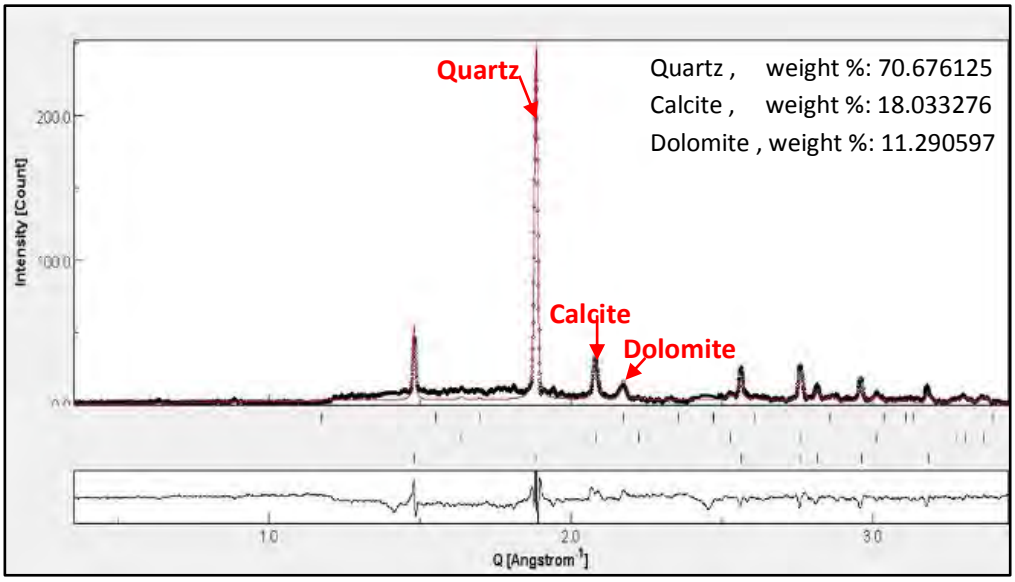

JA-23-1

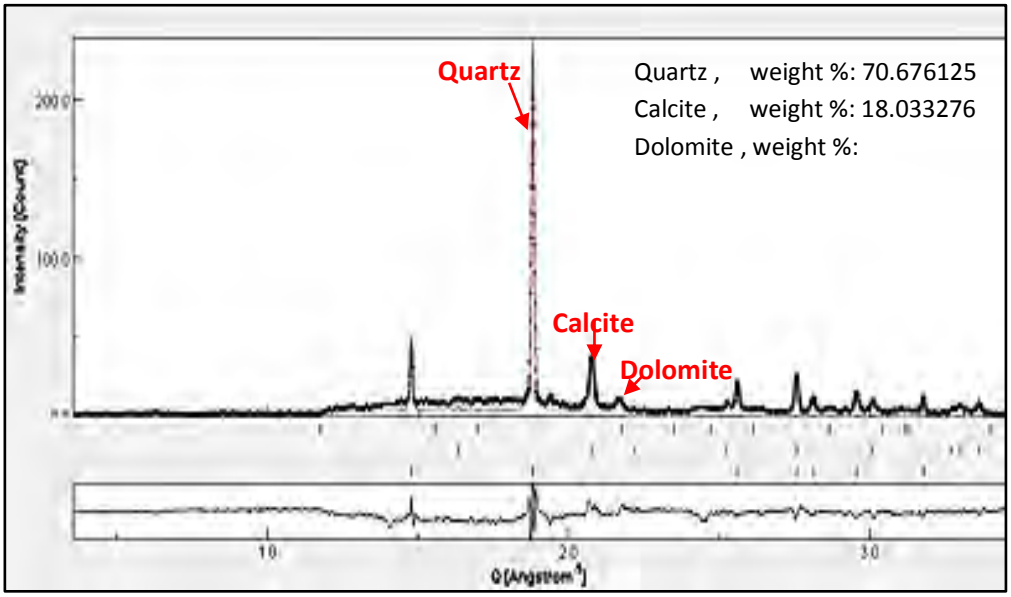

JA-23-2

Remark : JA-23-1: cutting sample from well JA-23 at depth 5500-5560 ft.

JA-23-2: cutting sample from well JA-23 at depth 5620-5680 ft

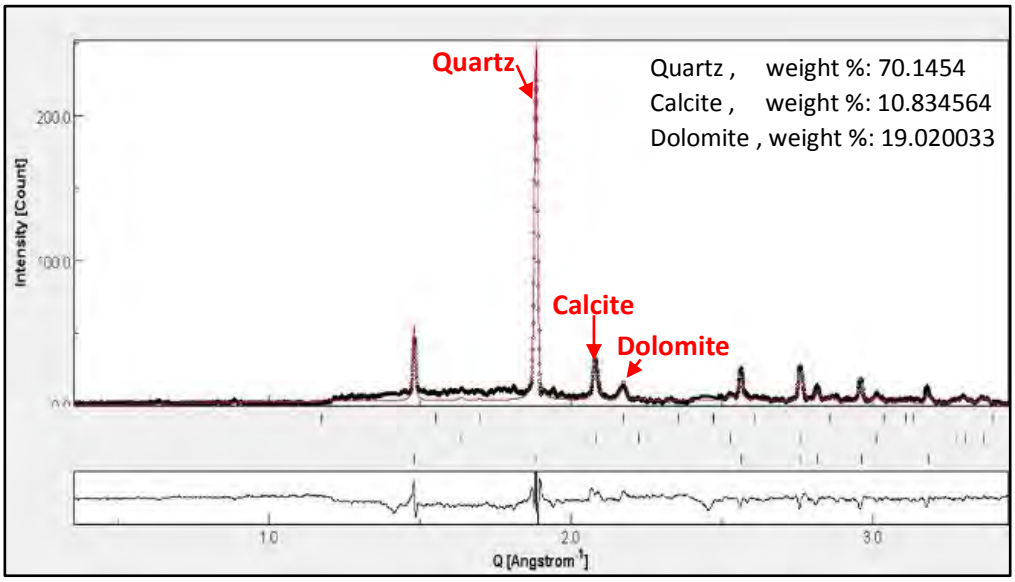

JA-23-3

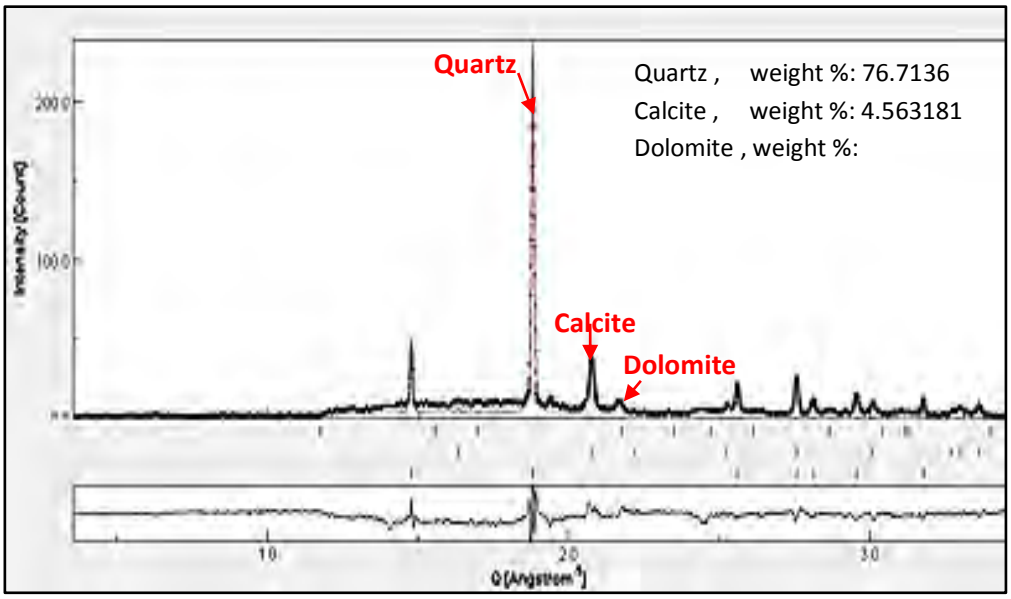

JA-23-4

Remark : JA-23-3: cutting sample from well JA-23 at depth 5860-5920 ft.

JA-23-4: cutting sample from well JA-23 at depth 6040-6100 ft.

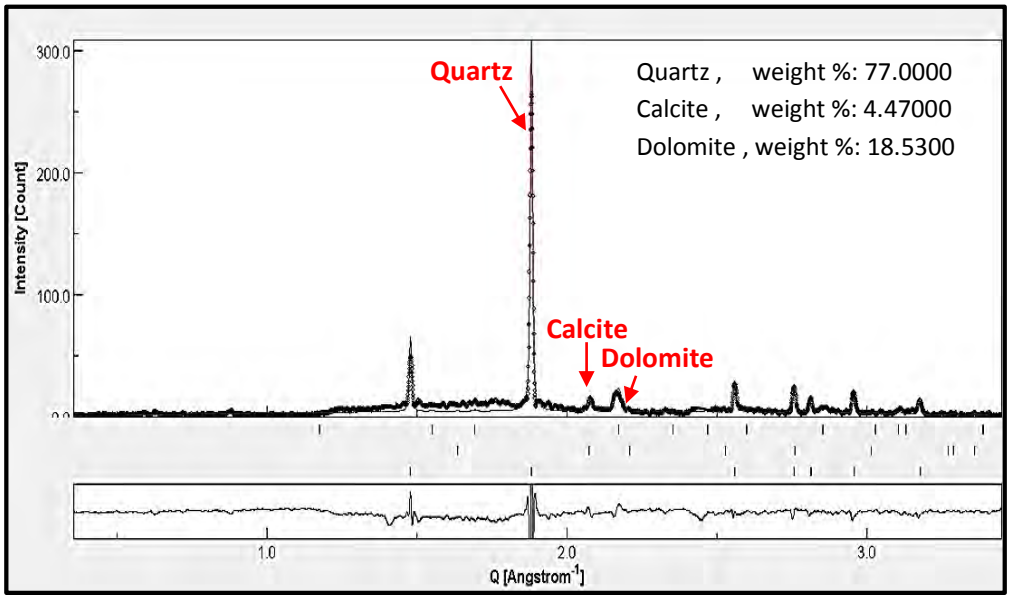

JA-23-5

Remark : JA-23-5: cutting sample from well JA-23 at depth 6220-6280 ft.

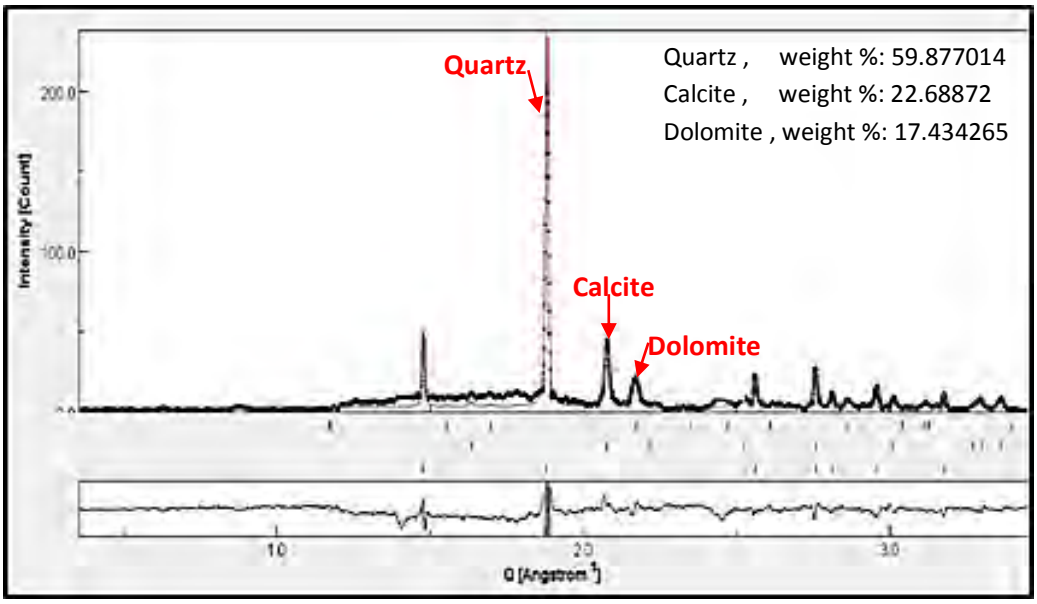

JA-27-1

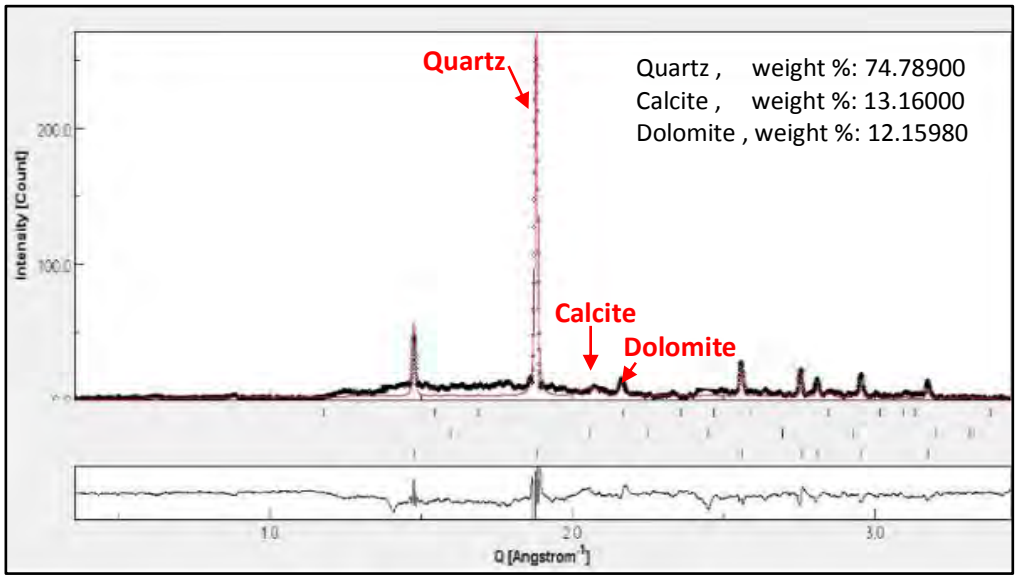

JA-27-2

Remark : JA-27-1: cutting sample from well JA-27 at depth 5020-5030 ft.

JA-27-2: cutting sample from well JA-27 at depth 5230-5260 ft

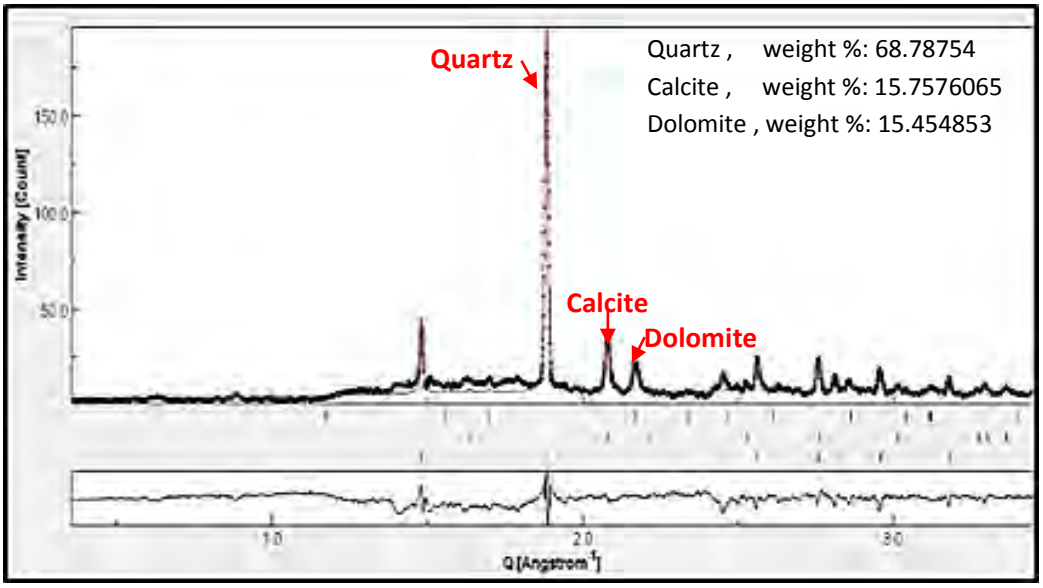

JA-27-3

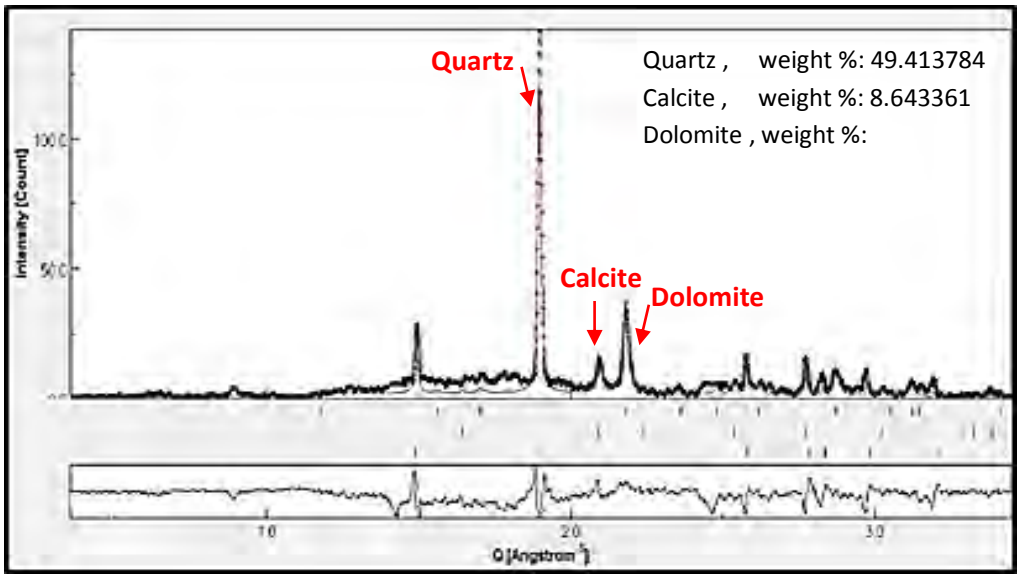

JA-27-4

Remark : JA-27-3: cutting sample from well JA-27 at depth 5380-5410 ft.

JA-27-4: cutting sample from well JA-27 at depth 5530-5560 ft.

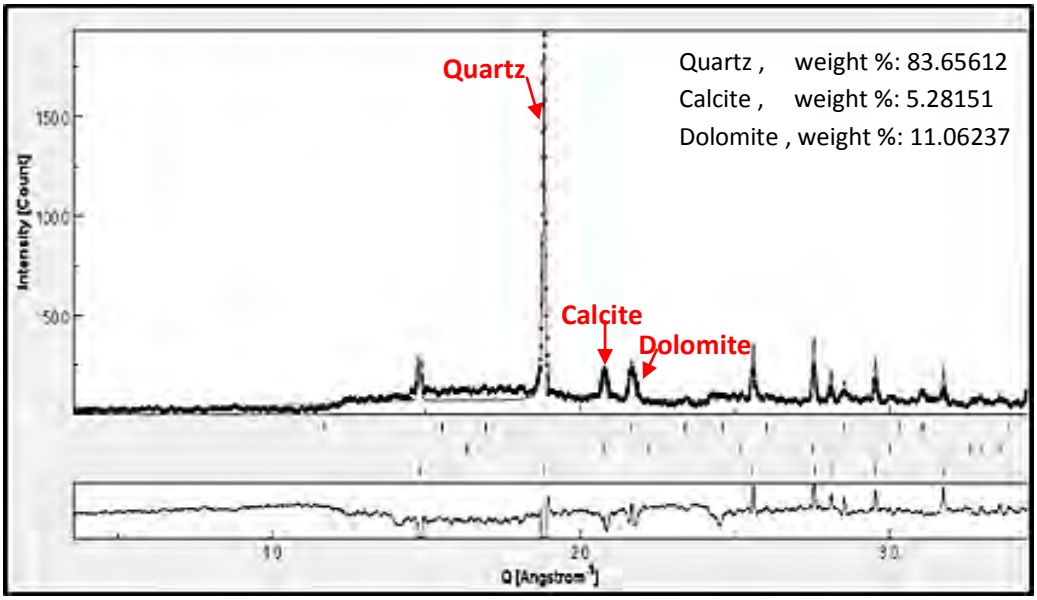

JA-27-5

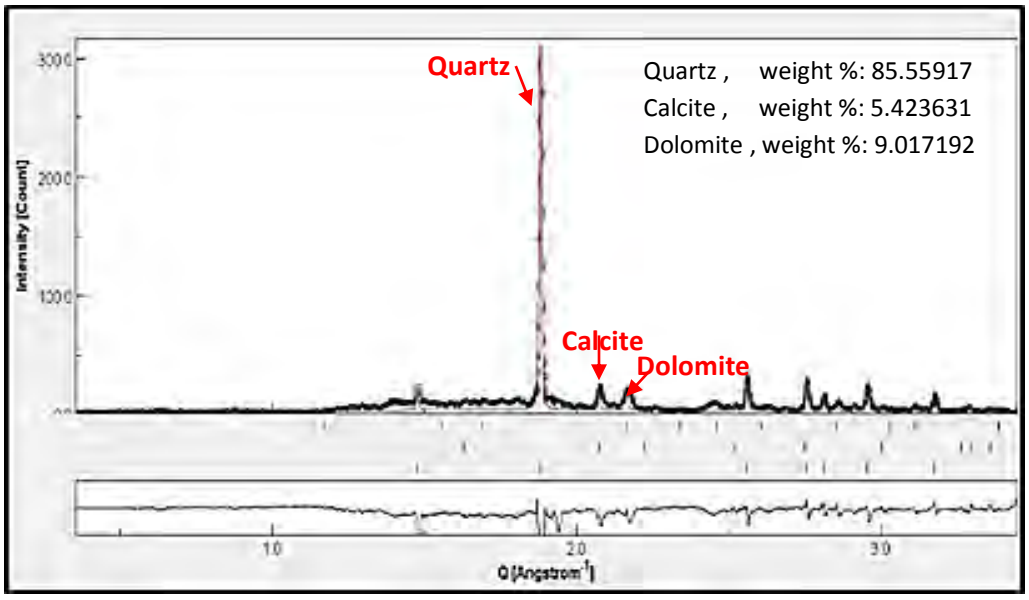

JA-27-6

Remark : JA-27-5: cutting sample from well JA-27 at depth 5710-5740 ft.

JA-27-6: cutting sample from well JA-27 at depth 6040-6070 ft.